

***Crystallization temperatures of tholeiite parental liquids:  
Implications for the existence of thermally driven mantle plumes***

**Trevor J. Falloon\***

*School of Earth Sciences and Centre for Marine Science, UTAS, Private Bag 79, Hobart,  
Tasmania 7001, Australia*

**David H. Green\***

*Research School of Earth Sciences, Australian National University, Canberra 0200, ACT,  
Australia*

**Leonid V. Danyushevsky\***

*School of Earth Sciences and ARC Centre for Excellence in Ore Deposits, UTAS, Private Bag  
79, Hobart, Tasmania 7001, Australia*

\*E-mails: [trevor.falloon@utas.edu.au](mailto:trevor.falloon@utas.edu.au); [David.H.Green@anu.edu.au](mailto:David.H.Green@anu.edu.au); [l.dan@utas.edu.au](mailto:l.dan@utas.edu.au)

**ABSTRACT**

**To compare magmatic crystallization temperatures between ocean island basalt (OIB) proposed to be plume-related and normal mid-ocean ridge basalt (MORB) parental liquids we have examined and compared in detail three representative magmatic suites from both ocean island (Hawaii, Iceland and Réunion) and mid-ocean ridge settings (Cocos-Nazca, East Pacific Rise, Mid-Atlantic Ridge). For each suite we have good data on both glass and olivine phenocryst compositions including volatile (H<sub>2</sub>O) contents. For each suite we have calculated parental liquid compositions at 0.2 GPa by incrementally adding olivine back into the glass compositions until a liquid in**

equilibrium with the most magnesian olivine phenocryst composition is obtained. The results of these calculations demonstrate that there is very little difference (max  $\sim 20$  °C) between the crystallization temperatures of the parental liquids (MORB 1243-1351 °C versus OIB 1286-1372 °C) when volatile contents are taken into account.

In order to constrain the depths of origin in the mantle for the parental liquid compositions we have performed experimental peridotite-reaction experiments at 1.8 and 2.0 GPa using the most magnesian of the calculated parental MORB liquids (Cocos-Nazca) and compared the others with relevant experimental data utilizing projections within the normative basalt tetrahedron. The mantle depths of origin determined for both the MORB and OIB suites are similar (MORB 1-2 GPa; OIB 1-2.5 GPa) using this approach.

Simple calculations of mantle potential temperatures ( $T_P$ 's) are sensitive to assumed source compositions and the consequent degree of partial melting. For fertile lherzolite sources,  $T_P$ 's for MORB sources range from 1318-1488 °C, whereas  $T_P$ 's for ocean-island tholeiite sources (Hawaii, Iceland and Réunion) range from 1502 °C (Réunion) to 1565 °C (Hawaii). The differences in  $T_P$ 's between the hottest MORB and ocean-island tholeiite sources are  $\sim 80$  °C, significantly less than predicted by the thermally driven mantle plume hypothesis. These differences disappear if the hot-spot magmas derive by smaller degrees of partial melting of a refertilized refractory source. Consequently the results of this study do not support the existence of thermally driven mantle plumes originating from the core-mantle boundary as the cause of ocean-island magmatism.

**Keywords:** MORB, Hawaii, Réunion, Iceland, Kilauea, olivine, peridotite melting experiments, mantle potential temperatures, primary magmas, mantle plumes.

## INTRODUCTION

The composition and temperature at which olivine crystallizes from a mantle-derived parental liquid at a low pressure is one of the key constraints on any model of magma genesis (e.g. Green and Ringwood, 1967; Sobolev and Danyushevsky, 1994), as these parameters are necessary for estimating potential temperatures of the source mantle. Olivine is the first phase to crystallize at low pressure from any mantle derived melt that is in chemical equilibrium with peridotite at source depths. This is due to the rapid expansion of the olivine phase volume at lower pressures, demonstrated by numerous experimental studies on model melt compositions. As both olivine crystallisation temperature and the composition of liquidus olivine are sensitive to the composition of the crystallising melt, it is possible to calculate both given the composition of melt alone. Conversely, given an olivine composition, it is possible to test whether an observed glass or rock composition is in equilibrium with the olivine, by using empirically calibrated functions for equilibria between melt and olivine end-members. Such a calibration is referred to as an olivine geothermometer (e.g., Roeder and Emslie, 1970; Ford et al., 1983; Herzberg and O'Hara, 2002).

The application of olivine geothermometry to determine the composition of parental liquids is of particular significance to our understanding of the causes of ocean island volcanism, including inferred hot mantle plumes. The hypothesis of thermally driven mantle plumes derived from the core-mantle boundary predicts a significant temperature contrast between upwelling plume material and ambient upper mantle. Consequently decompression melts derived from the mantle plume materials should be ~200-300 °C hotter than melts derived from ambient upper mantle (McKenzie and Bickle, 1988). If the thermally driven mantle plume hypothesis is correct then we should expect to find evidence from olivine crystallization temperatures that parental liquids to Hawaii olivine tholeiites, a typical ocean

island magma, are significantly hotter than parental liquids to mid-ocean ridge basalt (MORB) olivine tholeiites. We should also find evidence for very different pressures and degrees of partial melting. The determination of olivine crystallization temperatures of parental melts is also the first necessary step for estimating mantle potential temperatures ( $T_p$ 's).

In this paper we calculate the parental liquids for a representative range of tholeiite compositions from both mid-ocean ridge (Cocos-Nazca, East Pacific Rise, Mid-Atlantic Ridge) and ocean island settings (Hawaii, Réunion and Iceland). We find that there are no significant differences (max  $\sim 20$  °C) between crystallization temperatures of MORB and ocean island basalts (OIB) parental tholeiite liquids, when the hottest parental liquids from each setting are compared. In order to constrain the depth of origins in the mantle for the parental liquid compositions we have performed experimental peridotite-reaction experiments at 1.8 and 2.0 GPa (see appendix 1) using the most magnesian of the calculated parental MORB liquids (Cocos-Nazca) and compared the others with relevant experimental data utilizing projections within the normative basalt tetrahedron. The mantle depths of origin determined for both the MORB and OIB suites are similar (MORB 1-2 GPa; OIB 1-2.5 GPa) using this approach. Finally we present model calculations for the source mantle  $T_p$ 's of the calculated parental liquids. These calculations are significantly dependent on the chosen models of source compositions and thus on the inferred degree of partial melting and the magnitude of latent heat of melting in the models. Below we first outline the rationale of our approach before discussing in detail our case studies from Hawaii, Reunion, Iceland and MORB.

## **RATIONALE OF APPROACH**

Our approach to estimating the temperatures of tholeiite magmas is based on the use of olivine geothermometers to calculate the compositions of parental liquids. Unmodified parental liquids rarely erupt, and evidence for their existence is only preserved in the mineralogy of magnesian olivine phenocrysts enclosed in phyric magma (rock) compositions. An olivine geothermometer is therefore used to reconstruct the composition of the parental liquid, and its temperature of crystallisation, by adding back olivine in incremental equilibrium steps (e.g. 0.01 wt%, see appendix in Danyushevsky et al., 2000 for a detailed explanation) into an evolved liquid (glass) composition. This use of an olivine geothermometer assumes that olivine crystallises fractionally, i.e. olivine is chemically isolated from the melt when it is formed. Along with the assumption of fractional crystallization, the parental liquid calculation also requires the following:

1. A composition of an evolved melt within the olivine-only field. This should be either a natural glass composition or an aphyric whole-rock composition which represents a liquid.
2. To establish the composition of the most magnesian olivine phenocryst or microphenocryst for the suite, as a target for the olivine addition calculations. In any magma suite there will be found a range in olivine phenocryst compositions, if present (Danyushevsky et al., 2002). Most large olivine phenocrysts show normal zoning from core Mg# values ( $Mg\# = 100 * (X_{Mg} / (X_{Mg} + X_{Fe}))$ , where  $X_{Fe}$  and  $X_{Mg}$  are cation fractions of  $Fe^{2+}$  and Mg, respectively) higher than those in equilibrium with the erupted evolved liquid composition. Olivine in equilibrium with the erupted melt is usually present as both discrete microphenocrysts and rims on the more magnesian phenocryst cores. In some suites the magnesian olivine phenocrysts are xenocrystic and could either represent 1) disaggregated cumulate material from previously erupted magmas, which may or may not have similar magma compositions to

the composition of interest or 2) lithospheric wall rock samples detached and disaggregated as magmas or melts have moved through the lithosphere towards crustal magma chambers. Minor element (Ca, Al, Cr, Ni) or trace element contents of olivine may be used to evaluate phenocryst vs xenocryst relationships with respect to the host magma (Norman and Garcia, 1999). Also in most suites it is possible to identify and analyse melt inclusions in magnesian olivine phenocrysts which demonstrate that these olivine phenocrysts are related to the evolved liquid composition which has erupted, via the process of crystal fractionation. Where phenocryst and microphenocryst relationships are established, it is possible to use an olivine geothermometer to incrementally add back olivine in small equilibrium steps to obtain a parental composition that is in equilibrium with the most magnesian phenocryst composition observed (Irvine, 1977; Albarede, 1992; Danyushevsky et al., 2000).

3. An estimate of volatile content of the evolving melt (especially H<sub>2</sub>O) and its effect on the crystallisation temperature and composition. Anhydrous calculations for magmas which have small amounts of H<sub>2</sub>O can lead to large differences in crystallization temperatures between parental liquid compositions (e.g., Falloon and Danyushevsky, 2000). In this paper we use the model of Falloon and Danyushevsky (2000) to estimate the effect of H<sub>2</sub>O, on olivine liquidus temperatures. The effect of H<sub>2</sub>O on the value of the equilibrium constant for iron-magnesium exchange between olivine and liquid ( $K_D$ , defined as

$((X_{Fe})^{Ol}/(X_{Fe})^L)/((X_{Mg})^{Ol}/X_{Mg}^L)$ ; where Ol is olivine, L is melt,  $X_{Fe}$  and  $X_{Mg}$  are cation

fractions of Fe<sup>2+</sup> and Mg, respectively) is less well known but experimental and theoretical studies (Ulmer, 1989; Toplis, 2005; Putirka, 2005) suggest that the effect is very small for the likely H<sub>2</sub>O contents of tholeiite parental liquids (<1 wt%) and will not introduce a significant error into calculations by olivine geothermometers under anhydrous conditions.

4. An estimate of melt oxidation state. Two components are necessary, i) an oxygen fugacity and ii) a model to calculate the  $\text{Fe}^{2+}/\text{Fe}^{3+}$  ratio of the melt for the given oxygen fugacity (see Danyushevsky and Sobolev, 1996 for a detailed discussion). Differences in oxygen fugacity will not have a serious effect on conclusions reached about temperature differences between parental compositions ( $\sim 40^\circ\text{C}$  for four orders of magnitude difference in the oxygen fugacity).

5. An estimate of olivine crystallisation pressure. This can be determined from studies of primary fluid inclusions in olivine phenocrysts (e.g. Sobolev and Nikogosian, 1994; Anderson and Brown, 1993).

6. And finally the choice of an appropriate olivine geothermometer. In this paper we use the geothermometer of Ford et al. (1983) as this is the most appropriate for modelling olivine crystallization.

A more detailed review of the use of olivine geothermometers in calculating parental liquid compositions is provided by Falloon et al. (2006).

## **CASE STUDIES OF HOTSPOT OLIVINE THOLEIITE MAGMAS**

### ***Hawaii***

**Kilauea Volcano.** Kilauea is an active shield building volcano on the island of Hawaii. The magmatic rocks of Kilauea volcano have been the subject of a large number of detailed studies. These studies provide us with a relatively comprehensive set of data on

whole rocks, glass and olivine phenocryst compositions including volatile (H<sub>2</sub>O) contents. This makes Kilauea an ideal subject for our approach of calculating parental liquids for an ocean island tholeiite series. There are two aspects of the Kilauean data set which are of particular significance for our purposes. The first is the 1959 summit eruption of Kilauea, as this was a very intensely studied eruption both in terms of volcanology and petrology. The volcanological observations in particular recorded the height and temperatures of lava fountaining, and this data combined with associated petrological data on glasses and volatiles allows us to model the temperatures of eruptive magmas (see below). The second is the recovery of quenched glasses from the submarine Puna Rift (Clague et al., 1991; Clague et al., 1995). These glasses are the most magnesian (~15 wt% MgO) so far recovered for an ocean island tholeiite series. As well the Puna Rift glasses contain as microphenocrysts the most magnesian olivine compositions (Mg# 90.7) reported from Kilauea. Below we examine the 1959 eruption in detail to gain insights on likely volatile contents and pressures of olivine crystallization for Kilauea volcano. We then use the constraints derived from the 1959 eruption to examine the range of liquid compositions parental to the Puna Ridge glass compositions.

**Kilauea summit eruption of 1959.** The 1959 summit eruption lasted from 14<sup>th</sup> November to 20<sup>th</sup> December 1959 forming a cinder cone (Puu Puai) and a large lava lake in Kilauea Iki pit crater. The eruption consisted of 17 phases of high fountaining and lava output. Of particular importance is that observations were made of lava fountaining heights (max observed 580 m) and temperatures (using optical pyrometers; max observed fountain temperature 1190 °C, Ault et al., 1961), as well, the eruptive products of individual fountaining events were sampled. The most magnesian glass (S-5g, Table1) for a historical Kilauea eruption was sampled on the 18<sup>th</sup> November, 1959 from the hottest lava fountaining and the most olivine rich magma of the 1959 eruption (Murata and Richter, 1966). This

eruption on the 18<sup>th</sup> November provides us with a unique sample where we have a liquid composition and its eruption temperature (1190 °C). Using the olivine geothermometer of Ford et al. (1983) in combination with the model of Falloon and Danyushevsky (2000), we calculate a olivine liquidus temperature of 1190 °C, if the glass composition S-5g (also known as Iki-22 in some publications) was a liquid at 0.2 GPa containing 0.93 wt% H<sub>2</sub>O. This calculation was performed at 0.2 GPa as this is the maximum pressure of olivine crystallization for the 1959 eruption based on the study of primary CO<sub>2</sub> fluid inclusions by Anderson and Brown (1993). The volatile content is calculated so as to cause the appropriate liquidus depression to match the observed lava fountaining temperature, using the model of Falloon and Danyushevsky (2000) — in the absence of 0.93 wt% H<sub>2</sub>O, the calculated liquidus temperature for S5-g is 1261 °C i.e., 71 °C above the observed eruption temperature. This model volatile content results in a H<sub>2</sub>O/K<sub>2</sub>O value of 1.9375, close to the maximum observed values in olivine hosted melt inclusions from the eruption (Anderson and Brown 1993, see Figure 1) and values in the submarine Puna Ridge glasses (Clague et al., 1991; Clague et al., 1995). During crystal fractionation both H<sub>2</sub>O and K<sub>2</sub>O should be highly incompatible and thus should increase together in an evolving magma. The lack of correlation between H<sub>2</sub>O and K<sub>2</sub>O (Figure 1) indicates that significant degassing of H<sub>2</sub>O has occurred (Wallace and Anderson, 1998). It is therefore appropriate to take the higher H<sub>2</sub>O/K<sub>2</sub>O values as representative of the undegassed magma. Using the calculated H<sub>2</sub>O/K<sub>2</sub>O value for sample S-5g and applying it to the lowest MgO glass from this eruptive episode (sample F-3g, Table 1) we calculate a temperature of 1064 °C at 0.2 GPa, which closely matches the recorded temperature of the coolest fountains (1060 °C, Ault et al., 1961). In summary we believe that our modelling using the Ford et al. (1983) geothermometer in combination with the model of Falloon and Danyushevsky (2000) can accurately reproduce the eruption temperatures observed during the 1959-1960 eruptions of Kilauea volcano. We therefore use a pressure of

0.2 GPa and a H<sub>2</sub>O/K<sub>2</sub>O value of 1.9375 for the purposes of calculating parental liquid compositions to Kilauea volcano (see below).

**Puna Ridge Glasses.** In Figure 2 the FeO<sup>T</sup> and MgO contents of glasses recovered from the Puna Ridge are compared with glasses and whole rock compositions with >8.5 wt% MgO from Kilauea volcano. The blue arrow in Figure 2 delineates an olivine control line defined by the whole rock compositions of the 1959 summit eruption. This control line defines mixtures of variably fractionated liquids and olivine crystals with an average composition of ~Mg# 87 (Murata and Richter, 1966). The whole rock composition (S-5) for the glass S-5g was the most olivine rich magma of the 1959 eruption (Figure 2). As can be seen from Figure 2 the Puna Ridge glasses display a significant range in FeO<sup>T</sup> and MgO contents compared to the whole rock data analysed from Kilauea volcano. Four of the Puna Ridge glasses are of particular interest (Table 1). Sample 57-11c is the most magnesian glass of a high FeO<sup>T</sup> subset of glasses (Figure 2), whereas sample 57-9F is the only example of a relatively low FeO<sup>T</sup> glass. As can be seen from Figure 2, both the high and low FeO<sup>T</sup> glasses have no matching whole rock compositions. That is, so far no magma composition has been analysed from Kilauea volcano which is consistent with olivine accumulation into a high or low FeO<sup>T</sup> liquid composition. Glass samples 57-13g and 57-15D are important as they both contain olivine microphenocrysts (<20 μm) with core compositions ranging to Mg# 90.7, the most magnesian observed from Kilauea volcano. As the olivines are small microphenocrysts we can be reasonably confident that these microphenocryst have crystallized from a parental liquid related to the evolved glass composition. As well, both samples 57-13g and 57-15D have FeO<sup>T</sup> contents within the array defined by whole rock compositions from Kilauea volcano (Figure 2).

**Calculation of Parental melts for Kilauea Volcano.** In Table 2 and Figure 2 we present the results of parental liquid compositions at 0.2 GPa using a target olivine

composition of Mg# 90.7. We have performed calculations for S-5g and the four Puna Ridge glasses. Note that in Figure 2, the liquid lines of descent produced by adding olivine incrementally back into the glasses produce curved as opposed to straight lines. This emphasises the point made by Irvine (1977) and Albarede (1992) that extrapolation of olivine control lines (due to olivine accumulation) will result in incorrect calculated parental liquid compositions. Calculated parental compositions range in MgO contents from 14-18.8 wt% with crystallization temperatures ranging from 1286-1372 °C. As we do not know whether the target olivine is appropriate for both the high FeO<sup>T</sup> and low FeO<sup>T</sup> glasses, the most well constrained parental compositions are for glasses 57-13g and 57-15D. The parental liquids for these two compositions have 17-18 wt% MgO and crystallization temperatures of 1340-1355 °C.

**Mauna Loa Volcano.** The parental composition for Mauna Loa volcano was calculated in a similar manner to the Kilauea parental compositions. We used the most MgO rich glass recovered from the submarine southwest rift of Mauna Loa volcano (glass 182-7, Table 1). Sample 182-7 is particularly significant as it contains the most magnesian olivine phenocryst composition (Mg# 91.3) obtained from Mauna Loa volcano. Using this target olivine we calculate a parental liquid composition containing 17.53 wt% MgO at a temperature of 1354 °C (Table 2). As can be seen from Table 2, the parental liquid and temperature is essentially identical to those for samples 57-13g and 57-15D from Kilauea volcano. We believe that this result further supports the conclusion that samples 57-13g and 57-15D provide the most reliable estimates for Kilauea parental liquid compositions.

### ***Réunion***

**The 1939 eruption of Piton de la Fournaise.** The island of Réunion consists of two shield volcanoes, Piton des Neiges (3069 m) and Piton de la Fournaise (2631 m). The former is extinct and deeply eroded, whereas the latter is an active volcano. Picrites and olivine basalts from both volcanoes are referred to as the oceanite series. To model the composition of a parental magma for the oceanite series lavas of Réunion, we have chosen the melt composition from the oceanite magma eruption of the 6<sup>th</sup> January 1939, from Piton de la Fournaise volcano. The whole rock composition of the 1939 magma had 15.21 wt% MgO and the melt component of the magma, represented by glass REg has 7.18 wt% MgO (Table 1). The target olivine for our calculations is the most magnesian olivine phenocryst composition reported from the oceanite lavas of Réunion of Mg# 90.65 (Fretzdorff and Haase, 2002). H<sub>2</sub>O contents of olivine hosted melt inclusions in oceanite series lavas from Réunion suggest parental liquids have H<sub>2</sub>O/K<sub>2</sub>O values of ~2 (Figure 1, Bureau et al., 1988), essentially identical to Kilauea liquids. The calculated parental liquid to the REg glass composition at 0.2 GPa, has ~16 wt% MgO and a crystallization temperature of 1323 °C (Table 2), within the range calculated for parental liquids to Kilauea.

### ***Iceland***

**Theistareykir volcanic system NE Iceland.** The most magnesian olivine phenocryst composition that has been reported from Iceland has a Mg# of 92.4 (Sigurdsson et al., 2000). This olivine phenocryst comes from the Borgarhraun lava flow, which is part of the Theistareykir volcanic system and has an average whole rock MgO content of 12 wt% (MacLennan et al., 2003). The liquid composition is represented by glass NO42 which has 9.80 wt% MgO (Sigurdsson et al., 2000). The water content in this glass has not been analysed but can be estimated from its K<sub>2</sub>O content. Nichols et al. (2002) analysed H<sub>2</sub>O

contents of submarine and sub-glacial pillow basalts and concluded the Icelandic mantle source is relatively enriched in water. As can be seen from Figure 1, water contents in Icelandic lavas are very similar to Kilauea and Reunion. For the purposes of our calculation of a liquid composition parental to the glass NO42, we have used a  $H_2O/K_2O$  value of 2.5, which is close to the undegassed value for Icelandic magmas. The calculated parental liquid (Table 2) has 16.75 wt% MgO and a crystallization temperature of 1361 °C at 0.2 GPa.

## **COMPARISON BETWEEN 'HOTSPOT' AND SPREADING RIDGE THOLEIITES**

The thermally driven plume hypothesis predicts that there should exist a significant thermal anomaly between upwelling plume material and the temperature of ambient upper mantle. There is a general consensus that MORB are the result of melting from upwelling ambient upper mantle at oceanic spreading ridges. It would therefore seem a straightforward matter to compare parental liquid olivine crystallization temperatures between OIB and MORB. It is common in the literature to find the temperature of 1280 °C quoted and used as a sort of 'bench mark' for the  $T_p$  of the upwelling ambient upper mantle after the study of McKenzie and Bickle (1988). However it is important to recognize that this mantle  $T_p$  of 1280 °C represents an average, not the hottest MORB mantle  $T_p$ . Using this average temperature it would appear 'obvious' that a thermal anomaly exists. Indeed our own calculations for Kilauea volcano (Table 5) would indicate a thermal excess of ~285 °C, compared to an ambient upper mantle  $T_p$  of 1280 °C, a result consistent with the thermal plume hypothesis. We however strongly disagree with the use of an average temperature for MORB when there is clearly a range in olivine crystallization temperatures for MORB

glasses. This is demonstrated by the range in  $\text{FeO}^{\text{T}}$  versus MgO contents of MORB glasses (Figure 3). In Figure 3 we have plotted the  $\text{FeO}^{\text{T}}$  and MgO contents of 682 MORB glass analyses from the study of Danyushevsky (2001). These glass compositions were all determined by electron microprobe analysis using the glass standard VG-2 (USNM 111240/2, Jarosewich et al., 1980). Also plotted in Figure 3 are  $\text{FeO}^{\text{T}}$  and MgO contents of 189 glass compositions from the Petdb database ([petdb.ldeo.columbia.edu](http://petdb.ldeo.columbia.edu)). These 189 glasses were all determined by electron microprobe analysis (we note that many reported glasses in the Petdb database are in fact glass-rich rocks and whole rock analyses) and have MgO contents  $>9.5$  wt%. Consequently all these glasses (liquids) are in the olivine-only phase field at low-pressure. As can be seen from Figure 3 the MORB glasses from the two independent data sets display a significant range in  $\text{FeO}^{\text{T}}$  contents, and consequently there must exist a range in temperatures of MORB parental liquids. This is because if all calculation parameters are held constant, higher  $\text{FeO}^{\text{T}}$  contents require higher temperatures to be in equilibrium with the same olivine composition.

In this paper we wish to compare temperatures between the hottest of MORB parental liquids and the hottest of the OIB parental liquids, not averages. We believe it is appropriate to take the hottest of MORB parental liquids as representative of melts derived from adiabatic upwelling of ambient upper mantle. This is because there is a number of processes such as non-adiabatic upwelling, cooling, mantle-melt reaction etc. which could conceivably lead to lower temperatures in MORB parental liquids. If the lowest temperatures are taken as representative of ambient upper mantle, this provides no explanation for why hotter MORBs exist, apart from the circular argument that they are plume related and represent a depleted, MORB-source-like component within the plume. The discussion illustrates the difficulty of testing the deep mantle thermal plume hypothesis. In its most clearly stated form, the hypothesis asserts that spreading centres sample modern well-mixed upper mantle with N-

MORB trace element signatures . Mantle plumes sample compositionally distinct (OIB trace element and isotopic characteristics), heterogeneous mantle sources residing in the deep mantle. To the extent that these distinctions between magma and source characteristics are abandoned, the hypothesis requires modification or rejection. Just as circularity in argument is introduced if MORB-type (geochemically) and picritic magmas indicating high temperature are said to be influenced by or part of a nearby plume, it is similarly introduced with blurring of geochemical distinctions. The enriched, OIB-like geochemical signatures at many spreading centres with no obvious nearby plume are often attributed to a plume-component. For these reasons we have sought to establish magma temperatures and model mantle potential temperatures for the classical, geodynamically defined ‘fixed’ hot-spots and on geodynamically defined spreading centres, and the latter samples chosen for detailed scrutiny have N- or D-MORB geochemistry. Anticipating our possible conclusion, if we can find no significant temperature difference between parental MORB and hot-spot magmas, we seriously undermine the deep mantle thermal plume model but are left with the evidence for heterogeneous mantle, geochemical differences between MORB and OIB sources, and the hot-spot source/cause below and detached from the moving lithospheric plate.

In order to compare crystallization temperatures with MORB we have calculated parental liquid compositions at 0.2 GPa for three representative MORB glasses with differing  $\text{FeO}^{\text{T}}$  contents (Table 1, no. 9-11). These glasses are as follows:

- 1) the most magnesian glass (Table 1, no.9) from ODP site 896A, drilled into ~5Ma crust formed by the Cocos-Nazca spreading ridge (McNeill and Danyushevsky, 1996. herein referred to as ODP896A). This glass contains microphenocrysts with core compositions ranging to Mg# 91.6;

- 2) glass D20-3 (Table 1, no.10) from the Siqueiros Fracture Zone, East Pacific Rise (Danyushevsky et al., 2003). The most magnesian olivine phenocryst observed in the Siqueiros Fracture Zone has a Mg# of 91.5 and
- 3) the composition of a magnesian olivine-hosted glass inclusion from the Vema Fracture Zone on the Mid-Atlantic Ridge from the study of Sobolev et al. (1989). This glass inclusion composition is important as it is representative of a relatively low  $\text{FeO}^{\text{T}}$  liquid compared with the other parental MORB liquid compositions. The maximum olivine phenocryst composition observed in the Vema Fracture Zone has a Mg# of 90.5.

The  $\text{H}_2\text{O}$  contents listed in Table 1 have all been determined on the glasses themselves. In Table 3 and Figures 3 and 5 we present the results of our parental liquid calculations for all three compositions. The range in MgO contents in parental liquids range from ~10-16 wt% MgO and crystallization temperatures at 0.2 GPa range from 1243-1351 °C.

A significant result of our calculations (Table 2) is that the olivine crystallization temperature of the representative ODP896A parental liquid is significantly hotter than the commonly quoted ambient upper mantle  $T_p$  value of 1280 °C, and higher than the  $T_p$ 's inferred for MORB by Presnall et al. (2002), based on experimental studies on simple systems (average mantle potential temperature required ~1260 °C). We have chosen this particular high  $\text{FeO}^{\text{T}}$  MORB glass from ODP896A simply because we have detailed information on both mineralogy and geochemistry. Such detailed information required for our calculations is currently not available from the vast majority of studies which report MORB glass geochemistry. The ODP896A glass has normal N-MORB geochemistry (Danyushevsky, unpubl data) and we believe it is representative of other high  $\text{FeO}^{\text{T}}$  MORB glasses for which we do not have detailed information on mineralogy. Over half the glasses in the Petdb database (n=80) with MgO contents >9.5 wt% have  $\text{FeO}^{\text{T}}$  > 9 wt% similar to the ODP896A

glass. The average  $\text{FeO}^{\text{T}}$  of these high  $\text{FeO}^{\text{T}}$  ( $>9$  wt%) glasses is  $9.3\pm 0.3$ , thus the ODP896A glass ( $\text{FeO}^{\text{T}} = 9.1$ ) has slightly below average  $\text{FeO}^{\text{T}}$  compared to these glasses. These high  $\text{FeO}^{\text{T}}$  glasses are sampled from a range of 'normal' crustal thickness spreading ridges (Carslberg Ridge, Chile Ridge, Easter Microplate Rifts, East Pacific Rise, Galapagos Spreading Center, Juan De Fuca Ridge, Mid-Atlantic Ridge, Red Sea), and are associated with low  $\text{FeO}^{\text{T}}$  glasses both in time and space. Although primitive high MgO and high  $\text{FeO}^{\text{T}}$  glasses such as ODP896A are rarely sampled at spreading centers, glass compositions derived from such parents are relatively common. Dmitriev et al. (1985) using an eight-component discriminant function determined that at least 37% of MORB glasses from the Mid-Atlantic Ridge were derived from such high  $\text{FeO}^{\text{T}}$  parental compositions.

If we use our approach and calculate parental compositions for all the high MgO glasses ( $>9.5$  wt%,  $n=189$ ) from the Petdb database, using  $\text{K}_2\text{O}$  abundances as an estimate for  $\text{H}_2\text{O}$  contents and olivine target composition of Mg# 91.5, then calculated parental liquids at 0.2 GPa display a significant range in both MgO contents (13-18 wt%) and temperatures (1300-1430 °C), however the averages [ $15.1\pm 0.9$  wt% MgO;  $1343\pm 19$  °C] are very close to the calculated values for the ODP896A parental composition for which we have detailed petrological information. To determine the true range in composition and crystallization temperatures of MORB parental liquids requires more detailed petrological and mineralogical studies from a range of different spreading ridges. The uncertainty in calculations where only electron probe analyses of glass compositions are available is that we do not know the actual  $\text{H}_2\text{O}$  contents nor do we have any idea on the maximum Mg# of olivine phenocrysts. It may well be the case that we are underestimating the temperatures of some of the high  $\text{FeO}^{\text{T}}$  glasses, as some picrite suites with similar MORB geochemistry have olivines upto Mg# 93-94 (e.g. Baffin and Gorgona Island picrites). It is a circular argument which assigns these

high temperature picrite suites to the influence of mantle plumes, they may well be derived from normal ambient upper mantle.

In summary therefore we believe that when comparisons are made between olivine crystallization temperatures of parental liquids for OIB and MORB magmas, it is the temperatures inferred for parental liquids for high FeO<sup>T</sup> MORB glass suites which should be used to test the 'thermal plume hypothesis'. The result of our calculations suggest there are no significant differences in the olivine crystallization temperatures when OIB and MORB parental liquids are compared (the differences between MORB and the most well-constrained calculations for Kilauea volcano are essentially zero, and the Icelandic parent is only 10 °C hotter). If other picrite suites with MORB geochemistry are used in this comparison, then OIB parental liquids would be significantly cooler than MORB parental liquids.

## **MANTLE POTENTIAL TEMPERATURES**

As mentioned previously the calculation of parental liquid compositions is only the first step in the process of calculating a mantle  $T_p$ . In order to calculate mantle  $T_p$ 's it is necessary to make a number of assumptions concerning source compositions, mantle melting, and the melt segregation process. It is beyond the scope of this paper to present any comprehensive argument or defence of any particular mantle  $T_p$ . What we will do in this section is to present some simple mantle  $T_p$  calculations based on the following assumptions:

1. For comparative purposes, we first assume that the mantle sources for both OIB and MORB primary melts are of pyrolite composition, with bulk CaO and Al<sub>2</sub>O<sub>3</sub> contents within the range of ~3-4 wt%. We believe the assumption of a peridotitic (pyrolite) source is justified by the magnesian contents of both the calculated parental liquids and co-existing

olivines (Table 3). The production of primary melts of MgO contents of between 10-19 wt% MgO, and olivines of Mg# 90.5-92.4 requires an olivine-rich peridotite source. Many studies of Hawaiian volcanism however have argued the need for recycled crustal components in the mantle source in the form of eclogite and/or pyroxenite (Takahashi and Nakajima, 2002, Sobolev et al., 2005). However numerous experimental melting studies have demonstrated that eclogite and pyroxenite source components are incapable of producing any of the calculated parental liquids unless there has either been extensive reaction with peridotite before melt segregation (Green and Falloon, 2005), or alternatively mixing with a dominant peridotite melt component before eruption (Sobolev et al., 2005). In Figure 2 we have plotted the locus of  $\text{FeO}^{\text{T}}$  and MgO contents of initial melts (i.e., at the solidus) for both Hawaiian and MORB pyrolite compositions (Green and Falloon, 1998) using the equations of Herzberg and O'Hara (2002). Melts formed above the solidus by higher degrees of melting lie to the right of these lines. As can be seen from Figure 2 it is impossible for a MORB pyrolite composition source to produce melt compositions with appropriate  $\text{FeO}^{\text{T}}$  and MgO contents matching the calculated parental liquid compositions to Kilauea volcano. This observation was used as an argument by Herzberg and O'Hara (2002) for more magnesian parental liquids for Hawaii. For a mantle composition such as MORB pyrolite (7.55 wt%  $\text{FeO}^{\text{T}}$ ) to be a source for Kilauea parental liquids, MgO contents, in the case of the 57-13g parental liquid, would need to be >20 wt% MgO with olivine of >Mg# 91.9 at 0.2 GPa. So far there is no evidence for such magnesian olivine compositions from Hawaiian volcanoes. However if the mantle source has  $\text{FeO}^{\text{T}}$  and MgO contents similar to Hawaiian pyrolite composition (9.5 wt%  $\text{FeO}^{\text{T}}$ , Green and Falloon, 1998), then the calculated parental liquid compositions are possible primary melts of this mantle composition.

The Hawaiian pyrolite composition is believed to be a result of a complex history of previous melt extraction followed by mantle refertilization by small degree melts from

recycled subducted oceanic crust interacting with refractory lithosphere (harzburgite) and normal mantle (Yaxley and Green, 1998; Green and Falloon, 2005). We have previously suggested that, rather than the assumption that the source composition (Hawaiian pyrolite) should resemble the most fertile mantle-derived lherzolites with 3-4% CaO and Al<sub>2</sub>O<sub>3</sub> (Green and Falloon, 1998), and thus yield parental tholeiitic picrites by 30-40% melting (Table 5), a more appropriate source is a refertilized harzburgite with ~1.5-2 wt% CaO and Al<sub>2</sub>O<sub>3</sub> (Green et al., 2001). Such a harzburgitic source would be compositionally buoyant if at similar temperature to enclosing MORB pyrolite, and on upwelling would yield ~10% tholeiitic picrite with harzburgite residue. We therefore make alternative assumptions in our mantle T<sub>p</sub> calculations that either a very fertile lherzolite (Hawaiian pyrolite) or a refertilized harzburgite is a suitable mantle source composition for OIB primary melts. The two assumptions demonstrate the importance of the melt fraction and latent heat of melting estimates to calculation of mantle potential temperature. For MORB we assume a composition similar to peridotite MM-3 (Baker and Stolper, 1994) and MORB pyrolite (Green et al., 1979) as suitable mantle source compositions — both of these are lherzolite compositions with 3-4% CaO and Al<sub>2</sub>O<sub>3</sub>.

2. We assume that the melting process can be closely modelled by simple batch melting, and that the compositions of unmodified primary melts segregate from their mantle sources as a fully integrated and equilibrated melt compositions. Thus based on this assumption, we should be able to find at some P and T a close matching in composition between our calculated parental liquids and experimental melts from our assumed mantle source if the parental liquids are indeed primary mantle derived melts. Justification for this assumption is presented in Green and Falloon (1998) and in the case of Kilauea is supported by the petrogenetic model presented by Eggins (1992a, b). Our assumption of batch melting means

that we can simply calculate the degree of partial melting of our mantle source composition by using the abundances of the relatively incompatible minor elements  $\text{TiO}_2$ ,  $\text{Na}_2\text{O}$  and  $\text{K}_2\text{O}$  in our calculated parental liquids.

3. We ignore the possible effect of the relatively minor amounts of  $\text{H}_2\text{O}$  and  $\text{CO}_2$  which are contained in our calculated parental compositions, on the positions of mantle melting cotectics within the normative tetrahedron. We are not focussing on the C-H-O-controlled solidus and incipient melting regime but with the onset of the major melting regime (Green and Falloon, 1998, 2005). The main effect of  $\text{H}_2\text{O}$  is to produce a higher degree of partial melt at a given temperature compared to volatile free conditions. However when melt compositions are compared on an anhydrous basis, no significant differences are apparent both in the compositions of experimental melts nor their normative positions (for  $\text{H}_2\text{O} < 1\%$  approx in the melt).

4. We assume that the mantle source upwells adiabatically and that when it crosses its solidus undergoes partial melting. This is a very important assumption as mantle  $T_p$  calculations presented will be in error if upwelling is not adiabatic (c.f., Ganguly, 2005). For these models of tholeiitic picrite genesis we assume that the 'solidus' is actually the entry into the 'major melting regime of the peridotite-C,H,O' system (see 3 above and Green and Falloon, 1998, 2005, Figure 3).

5. To calculate the amount of heat loss due to melting of the mantle source we have used the values for the latent heating of melting (100 cal/gm) and heat capacity (0.3 cal/gm/deg) recommended by Langmuir et al. (1992). For the two alternative source compositions (Iherzolite and harzburgite) for Hawaiian or other hot-spot magmas, the heat loss calculated

is very different such that  $\frac{dT_p}{dF}$  for different melt fractions is approx 3.3 °C per 1% melt (Table 5).

6. We assume a mantle solid adiabat of 10 °C/GPa (Birch, 1952) and liquid adiabat of 30 °C/GPa (McKenzie and Bickle, 1988).

### ***Depths of mantle equilibration***

In order to determine mantle depths of mantle equilibration of our calculated parental liquids we have projected their compositions from both olivine and diopside end-members into the normative tetrahedron and compared them with experimentally determined mantle melting cotectics (Figures 4 and 5, Tables 3 and 4). In Table 5 we also present a pressure of mantle equilibration using the experimentally calibrated empirical model of Alabarede (1992). Both methods give reasonably consistent results.

**Kilauea volcano.** In Figure 4 the glasses and parental compositions from Kilauea are shown projected from olivine (Figure 4A) or diopside (Figure 4B) and compared with experimentally determined cotectics on the Hawaiian Pyrolite composition. Green and Falloon (2005) have previously shown that compositions from a range of Hawaiian volcanoes define arrays of compositions in the olivine projection consistent with equilibrium with harzburgite residues but with differing Ca/Al ratios. In Figure 4A it can be seen that the mantle source for the 1959 Kilauea summit eruption must have a higher Ca/Al value compared to the source for the Puna Ridge glasses and other historical eruptions of Kilauea (e.g. data of Norman and Garcia 1999, Norman et al., 2002). The Hawaiian pyrolite was based on the 1959 eruption compositions and thus the Ca/Al ratio of Hawaiian pyrolite matches the S-5g glass in Figure 4A but is too high for the Puna Ridge glasses.

In Figure 4B the calculated parental compositions show a range of mantle equilibration pressures from ~1 GPa (57-9F) to 2.5 GPa (57-11c). The two most well constrained parental compositions (57-13g and 57-15D) are both consistent with a pressure of ~2 GPa and closely match experimental compositions from Hawaiian Pyrolite at this pressure (Table 3). This pressure of mantle equilibration matches the expected pressure at the base of the oceanic lithosphere (~60km) beneath Hawaii based on geophysical studies (Eaton and Murata, 1960). Thus the parental liquid compositions calculated for 57-13g and 57-15D are consistent with the model in which a compositionally buoyant diapir (i.e. plume) is emplaced into the base of the oceanic lithosphere, and melt fractions are integrated and equilibrated with a harzburgite residue before segregation via melt channelling through the oceanic lithosphere to crustal magma reservoirs at ~0.2 GPa (~6km) depth beneath Kilauea volcano. In such a model the garnet signature observed in Hawaiian magmas is either the result of the integration of very small melt fractions derived from equilibrium with garnet over a range of pressures (Eggins, 1992a, b) or is a source feature derived by reaction between melts derived from the incipient melting of eclogite and refractory harzburgite (Yaxley and Green, 1998).

However the low Fe (57-9F) and high Fe (57-11c) glasses are inconsistent with this model. The calculated parental compositions to these glasses indicate pressures of ~1 GPa for 57-9F and ~2.5 GPa for 57-11c. It is very difficult to relate the differences in inferred pressures of mantle equilibration to any known mantle melting or reaction process as both these glasses are colinear with glasses 57-13g and 57-15D in the projection from olivine in Figure 4A. That is, all the Puna Ridge parental glass compositions define a single olivine control line in both Figure 4A and Figure 4B, whereas Figure 2 indicates that it is impossible for them to be related by olivine fractionation due to their strong differences in  $\text{FeO}^T$  content. Some process other than mantle melting or reaction must be invoked to explain the compositions of glasses 57-11c and 57-9F. As both these glass compositions have no known

matching whole rock compositions, we consider them to be anomalous and therefore mantle  $T_p$  calculated for their parental liquids should be treated with caution.

**Mauna Loa.** The parental composition to the glass 182-7 is also consistent with a mantle equilibration pressure of 2 GPa. This further supports the view that 2 GPa represents the pressure at the base of the oceanic lithosphere and that major element compositions of parental liquids reflect equilibration with a harzburgite mantle source at this pressure.

**Réunion and Iceland.** Both parental compositions give depths of mantle equilibration of ~2.5 GPa (Figure 4B, Figure 5B).

**MORB.** In Figure 5 we compare the parental compositions of our three representative MORB glass compositions with experimentally determined cotectics from melting experiments on peridotite composition MM-3 and MORB pyrolite. The parental compositions define a range of pressures (~1-2 GPa, Table 5) correlated with their  $\text{FeO}^T$  contents. In particular the calculated parental composition to the glass ODP896A shows a very close matching to experimental reaction compositions using the parental composition for the same glass calculated by McNeill and Danyushevsky (1996) and peridotite MM-3 (Table 4, Appendix 1). This result gives support to the assumption that mantle melting can be modelled by simple batch melting, and that major elements of primary melts reflect the pressure of last equilibration with the mantle and do not represent a mixture of independent melt fractions finally assembled in a crustal magma chamber.

**Summary.** The results of this study based on reasonable assumptions concerning source compositions and melting processes, indicates very little differences in pressures of mantle equilibration between MORB and OIB parental liquids (1-2 GPa verses 1-2.5 GPa). We have used the mantle equilibration pressures and the models of Ford et al. (1983) and Falloon and Danyushevsky (2000) to calculate temperatures of equilibration with olivine at the pressures indicated from the normative tetrahedron analysis. These temperatures are listed

in Table 5 ( $T_{\text{final}}$ ). As was the case with temperatures at 0.2 GPa, there is very little difference in temperatures between these parental compositions derived from similar pressures of mantle equilibration. The most well constrained compositions from Kilauea and Mauna Loa give temperatures and pressures of mantle equilibration essentially identical to the hottest MORB composition ODP896A (1422-1451 °C versus 1441 °C). These results strongly suggest that there is unlikely to be any significant differences in source mantle  $T_p$  between OIB and MORB.

### **Calculation of mantle $T_p$ 's**

Based on the assumptions listed previously (see above) we present in Table 5 our results of mantle  $T_p$  calculations for the calculated parental compositions. The highest calculated MORB source  $T_p$  is 1488 °C, for Réunion 1502 °C, for Iceland 1501 °C and the most well-constrained estimate for Hawaii is 1565 °C. These simple but non-unique results demonstrate that there does not exist a significantly large difference in mantle  $T_p$  between OIB and MORB mantle. If the degree of melting for Hawaii is the lower of the values presented in Table 5, due to a more refractory source than Hawaiian pyrolite, then the  $T_p$  differences between OIB and MORB source mantle would be essentially zero.

### **CONCLUSIONS**

In this study we have modelled the reverse of olivine fractionation to calculate parental liquids for a range of OIB and MORB glasses. Our results suggest there is very little difference in either the temperature of crystallization or the pressure and temperature of mantle equilibration between parental liquids in OIB and MORB settings. This result

strongly suggests that it is unlikely that there is a significant difference in source mantle  $T_P$ 's. This is supported by simple non-unique calculations of mantle  $T_P$ 's based on a number of reasonable assumptions.

## **ACKNOWLEDGMENTS**

We thank Kaj Hoernle, Mike Walter, Gillian Foulger and Donna Jurdy for their constructive reviews of this paper.

## **APPENDIX 1. EXPERIMENTAL PERIDOTITE-REACTION EXPERIMENTS ON A MODEL PARENTAL LIQUID COMPOSITION AT 1.8 AND 2.0 GPA.**

### **INTRODUCTION**

In this appendix we present experimental results (Tables A1-A3) of peridotite reaction experiments between peridotite MM-3 (Baker and Stolper, 1984) and the parental liquid to glass ODP896A (glass ODP Leg 896A-27R-1, 124-130, pc.15, calculated by McNeill and Danyushevsky, 1996 at 0.01 MPa) at 1.8 and 2.0 GPa. At 2.0 GPa we also present the results of reaction experiments using the magnesian MORB composition ARP74 10-16 (Bougault et al., 1979).

### **EXPERIMENTAL AND ANALYTICAL TECHNIQUES**

The starting compositions (ODP896A, ARP74 and MM-3, Table A1) were prepared from a mixture of analytical grade oxides and carbonates (Ca, Na), ground under acetone in

an agate mortar. This mixture was pelletised and sintered overnight (~16-20 hours) at 950 °C. An appropriate amount of synthetic fayalite was then added to the sintered mix and the mixture was again ground under acetone, before storage in glass vials in a 110 °C oven. Experiments were performed using standard piston-cylinder techniques in the High Pressure Laboratory formerly housed in the School of Earth Sciences, University of Tasmania. Experiments all used NaCl/Pyrex assemblies with graphite heaters, fired pyrophyllite and alumina spacers, mullite and alumina surrounds, graphite capsules and a W<sub>97</sub>Re<sub>3</sub>/W<sub>75</sub>Re<sub>25</sub> thermocouple. The thermocouple enters the assembly through a composite two and four bore-alumina sheath. The thermocouple was separated and protected from the graphite capsule by a 1mm alumina disc. No pressure correction was applied to the thermocouple calibration. The thermocouple junction is formed by crossing the thermocouple wires utilizing the four bore-alumina sheath which forms the top 5mm of the alumina thermocouple sheath. All experimental components and starting materials were stored in a oven at 110 °C. Experiments were performed using the hot piston-out technique and pressures are accurate to within ±0.1 GPa. Temperature was controlled to within ±1 °C of the set point using a Eurotherm type 818 controller.

At the end of each experiment the entire experimental charge was mounted and sectioned longitudinally before polishing. Experimental run products were analysed either by wave length dispersive microanalysis using Cameca SX-50 microprobes housed in the Central Science Laboratory, University of Tasmania (operating conditions 15 KV, 20 nA) or energy dispersive microanalysis using a Cameca MICROBEAM microprobe housed in the Research School of Earth Sciences, The Australian National University (operating conditions 15 KV, 5 nA). All glass analyses have been normalized to the composition of international glass standard VG-2 (Jarosewich et al., 1980) which was analysed together with the glasses under the same analytical conditions.

Our experimental results are presented in Tables A2 and A3. In Table A3 electron microprobe analyses of selected run products and mass balance calculations are presented. Table A3 demonstrates that our run products are essentially homogeneous and produce good mass balance with low sums of residuals squared. Our run times of 24 hrs are sufficient to have produced experimental run products closely matching equilibrium assemblages for the respective bulk compositions used.

#### **REFERENCES CITED**

Albarede, F., 1992. How deep do common basaltic magmas form and differentiate?: *Journal of Geophysical Research*, v. 97, p. 10,997-11,009.

Anderson, A. T., and Brown G. G., 1993, CO<sub>2</sub> and formation pressures of some Kilauean melt inclusions: *American Mineralogist*, v. 78, p. 794-803.

Aramaki, S., and Moore, J. G., 1969, Chemical composition of prehistoric lavas at Makaopuhi Crater, Kilauea Volcano, and periodic change in alkali content of Hawaiian tholeiitic lavas: *Bull Earthquake Res Inst*, v. 47, p. 257-270.

Ault, W. U., Eaton, J.P., and Richter, D.H., 1961, Lava temperatures in the 1959 Kilauea eruption and cooling lake: *Geological Society America Bulletin*, v. 72, p. 791-794.

Baker, M.B., and Stolper, E. M., 1994. Determining the compositions of high-pressure melts using diamond aggregates: *Geochimica et Cosmochimica Acta*, v. 58, p. 2811-2827.

Basaltic Volcanism Study Project, 1981, Basaltic Volcanism on the Terrestrial Planets.  
Pergamon Press, Inc., New York. 1286 pp.

Birch, F., 1952, Elasticity and constitution of the earth's interior: *Journal of Geophysical Research*, v. 57, p. 227-286.

Borisov, A.A., and Shapkin, A.I., 1990, A new empirical equation relating  $Fe^{3+}/Fe^{2+}$  in magmas to their composition, oxygen fugacity, and temperature: *Geochemistry International*, v. 27, p. 111-116.

Bougault, H., Cambon, P., Corre, O., Joron, J.L., and Treuil, M., 1979, Evidence for variability of magmatic processes and upper mantle heterogeneity in the axial region of the Mid-Atlantic Ridge near 22°N and 36°N: *Tectonophysics*, v. 55, p. 11-34.

Bureau, H., Pineau, F., Métrich, N., Semet, M.P., and Javoy, M., 1998, A melt and fluid inclusion study of the gas phase at Piton de la Fournaise volcano (Réunion Island): *Chemical Geology*, v. 147, p. 115-130.

Chen, C.-Y., Frey, F.A., Rhodes, J.M., and Easton, R.M., 1996, Temporal geochemical evolution of Kilauea Volcano: comparison of Hilina and Puna Basalt: *Earth Processes*, in, Basu, A., and Hart, S.R., eds., *Reading the Isotopic Code*, Geophysical Monogram 95, p.161-181.

Clague, D. A., Weber W.S., and Dixon, J.E., 1991, Picritic glasses from Hawaii: *Nature*, v. 353, p. 553-556.

Clague, D.A., Moore, J.G., Dixon, J.E., Friesin, W.B., 1995, Petrology of submarine lavas from Kilauea's Puna Ridge, Hawaii: *Journal of Petrology*, v. 36, 299-349.

Danyushevsky, L. V., 2001, The effect of small amounts of H<sub>2</sub>O on crystallization of mid-ocean ridge and backarc basin magmas: *Journal of Volcanology and Geothermal Research*, v. 110, p. 265-280.

Danyushevsky, L.V., and Sobolev, A.V., 1996, Ferric-ferrous ratio and oxygen fugacity calculations for primitive mantle-derived melts: calibration of an empirical technique: *Mineralogy and Petrology*, v. 57, p. 229-241.

Danyushevsky, L.V., Della-Pasqua, F.N., and Sokolov, S., 2000, Re-equilibration of melt inclusions trapped by magnesian olivine phenocrysts from subduction-related magmas: petrological implications: *Contributions to Mineralogy and Petrology*, v. 138, p. 68-83.

Danyushevsky, L.V., Sokolov, S., and Falloon, T.J., 2002, Melt inclusions in olivine phenocrysts: using diffusive re-equilibration to determine the cooling history of a crystal, with implications for the origin of olivine-phyric volcanic rocks: *Journal of Petrology*, v. 43, p. 1651-1671.

Danyushevsky, L.V., Perfit, M.R., Eggins, S.M., and Falloon, T.J., 2003, Crustal origin for coupled 'ultra-depleted' and 'plagioclase' signatures in MORB olivine-hosted melt inclusions: evidence from the Siqueiros Transform Fault, East Pacific Rise: *Contributions to Mineralogy and Petrology*, v. 144, p. 619-637.

Dmitriev, L.V., Sobolev, A.V., Sushevskaya, N.M., and Zpunny, S.A., 1985, Abyssal glasses, petrologic mapping of the oceanic floor and "geochemical Leg" 82, in Bougault, H., Cande, S.C. et al., Initial Reports of the Deep Sea Drilling Project, vol LXXXII, Washington (U.S. Government Printing Office), p. 509-518.

Eaton, J.P. and Murata, K.J., 1960, How volcanoes grow: *Science*, v. 132, p. 925-938.

Eggins, S. M., 1992a, Petrogenesis of Hawaiian tholeiites: 1, phase equilibria constraints: *Contributions to Mineralogy and Petrology*, v. 110, p. 387-397.

Eggins, S. M., 1992b, Petrogenesis of Hawaiian tholeiites: 2, aspects of dynamic melt segregation: *Contributions to Mineralogy and Petrology*, v. 110, p. 398-410.

Falloon, T.J., and Green, D.H., 1998, Anhydrous melting of peridotite from 8 to 35kb and the petrogenesis of MORB: *Journal of Petrology, Special Lithosphere Issue*, p.379-414.

Falloon, T.J., Green, D.H., Hatton, C.J., and Harris, K.L., 1988, Anhydrous partial melting of fertile and depleted peridotite from 2 to 30 kbar and application to basalt petrogenesis: *Journal of Petrology*, v.29, p.257-282.

Falloon, T. J., Green, D.H., Danyushevsky, L.V., and Faul, U. H., 1999, Peridotite Melting at 1.0 and 1.5 GPa: an Experimental Evaluation of Techniques using Diamond Aggregates and Mineral Mixes for Determination of Near-solidus Melts: *Journal of Petrology*, v. 40, p. 1343-1375.

Falloon, T.J., Danyushevsky, L.V., 2000, Melting of refractory mantle at 1.5, 2 and 2.5 GPa under anhydrous and H<sub>2</sub>O-undersaturated conditions: Implications for high-Ca boninites and the influence of subduction components on mantle melting: *Journal of Petrology*, v. 41, p. 257-283.

Falloon, T.J., Danyushevsky, L.V., and Green, D.H., 2001, Reversal experiments on partial melt compositions produced by peridotite-basalt sandwich experiments: *Journal of Petrology*, v. 42, p. 2363-2390, doi: 10.1093/petrology/42.12.2363.

Falloon, T.J., Danyushevsky, L.V., Ariskin, A., Green, D.H., and Ford, C.E., 2006, The application of olivine geothermometry to infer crystallization temperatures of parental liquids: implications for the temperature of MORB magmas: *Chemical Geology special issue* (in press).

Ford, C. E., Russell, D.G., Craven, J.A., and Fisk, M.R., 1983, Olivine-liquid equilibria: Temperature, pressure and composition dependence of the crystal/liquid cation partition coefficients for Mg, Fe<sup>2+</sup>, Ca and Mn: *Journal of Petrology*, v. 24, p. 256-265.

Fretzdorff, S., and Haase, K.M., 2002, Geochemistry and petrology of lavas from the submarine flanks of Reunion Island (western Indian Ocean): implications for magma genesis and the mantle source: *Mineralogy and Petrology*, v. 75, p. 153-184.

Ganguly, J., 2005, Adiabatic decompression and melting of mantle rocks: an irreversible thermodynamic analysis: *Geophysical Research Letters*, v.32, LO6312, doi: 10.1029/2005GL022363.

Garcia, M.O., Rhodes, J.M., Wolfe, E.W., Ulrich, G.E., and Ho, R.A., 1992, Petrology of lavas from episodes 2-47 of the Pu'u O'o eruption of Kilauea Volcano, Hawaii: evaluation of magmatic processes: *Bulletin of Volcanology*, v. 55, p. 1-16.

Garcia, M. O., Hulsebosch, T.P., and Rhodes, J.M., 1995, Olivine-Rich Submarine Basalts from the Southwest Rift Zone of Mauna Loa Volcano: Implications for Magmatic Processes and Geochemical Evolution. In: Rhodes, J. M., and Lockwood, J.P., eds., *Mauna Loa Revealed: Structure, Composition, History, and Hazards*, Geophysical Monograph 92, p. 219-239.

Garcia, M.O., Rhodes, J.M., Trusdell, F.A., and Pietruszka, A.J., 1996, Petrology of lavas from the Pu'u O'o eruption of Kilauea Volcano: III. The Kupaianaha episode (1986-1992): *Bulletin of Volcanology*, v. 58, p. 359-379.

Garcia, M.O., Ito, E., Eiler, J.M., and Pietruszka, A.J., 1998, Crustal contamination of Kilauea Volcano magma revealed by oxygen isotope analysis of glass and olivine from Pu'u O'o eruption lavas: *Journal of Petrology*, v. 39, p. 803-817.

Garcia, M.O., Pietruszka, A.J., Rhodes, J.M., and Swanson, K., 2000, Magmatic processes during the prolonged Pu'u O'o eruption of Kilauea Volcano, Hawaii: *Journal of Petrology*, v. 41, p. 967-990.

Garcia, M.O., Pietruszka, A.J., and Rhodes, J.M., 2003, A petrologic perspective of Kilauea Volcano's summit magma reservoir: *Journal of Petrology*, v.44, p. 2313-2339.

Green, D. H., and Ringwood, A.E., 1967, The genesis of basaltic magmas: *Contributions to Mineralogy and Petrology*, v. 15, p. 103-190.

Green, D.H., and Falloon, T.J., 1998, Pyrolite: A Ringwood concept and its current expression, in Jackson, I.N.S., ed., *The Earth's mantle: Composition, structure, and evolution*: Cambridge, England, Cambridge University Press, p. 311-380.

Green, D. H., and Falloon, T.J., 2005, Primary magmas at mid-ocean ridges, “hot spots” and other intraplate settings: Constraints on mantle potential temperature, in Foulger, G.R., Natland, J.H., Presnall, D.C., and Anderson, D.L., eds., *Plates, Plumes and Paradigms*. Geological Society of America Special Paper 388, p.217-247, doi: 10.1130/2005.2388(14)

Green, D. H., Falloon, T.J., Eggins, S.E., and Yaxley, G.M., 2001, Primary magmas and mantle temperatures: *European Journal of Mineralogy*, v. 13, p. 437-451.

Gunn, B.M., 1971, Trace element partitioning during olivine fractionation of Hawaiian basalts: *Chemical Geology*, v.8, p. 1-13.

Helz, R.T., 1980, Crystallization of Kilauea Iki lava lake as seen in drill core recovered in 1967-1979: *Bulletin of Volcanology*, v. 43, p. 675-701.

Helz, R. T., 1987, Diverse Olivine Types in Lava of the 1959 Eruption of Kilauea Volcano and Their Bearing on Eruption Dynamics In: Dekker, R. W., Wright T.L. and Stauffer, P.H. eds Volcanism in Hawaii, Geological Survey of America Professional Paper 1350, p. 691-722.

Herzberg, C., and O'Hara, M.J., 2002. Plume-associated ultramafic magmas of Phanerozoic Age: *Journal of Petrology*, v. 43, p. 1857-1883.

Irvine, T.N., 1977, Definition of primitive liquid compositions for basic magmas: *Year Book Carnegie Inst. Washington*, 76, 454-461.

Jarosewich, E.J., Nelen, J.A., and Norberg, J.A., 1980, Reference samples for electron microprobe analyses: *Geostandards Newsletter*, v. 4, p. 257-258.

Klein, E.M., Langmuir, C.H., 1987, Global correlations of ocean ridge basalt chemistry with axial depth and crustal thickness: *Journal of Geophysical Research*, v. 92, p. 8089-8115.

MacDonald, G. A., and Eaton, J.P., 1955, Hawaiian Volcanoes during 1953: *United States Geological Survey Bulletin*, v. 1021-D, p. 127-166.

Mangan, M.T., Heliker, C.C., Hofmann, A.W., Mattox, T.N., Kauahikaua, J.P., and Helz, R.T., 1995, Episode 49 of the Pu'u O'o-Kupaianaha eruption of Kilauea Volcano: breakdown of a steady-state eruptive area: *Bulletin of Volcanology*, v. 57, p. 127-135.

Maclennan, J., McKenzie, D., Hilton, F., Gronvöld, K., and Shimizu, N., 2003, Geochemical variability in a single flow from northern Iceland: *Journal of Geophysical Research*, v. 108, No. B1, 2007, doi:10.1029/2000JB000142.

McKenzie, D., and Bickle, M.J., 1988, The volume and composition of melt generated by extension of the lithosphere: *Journal of Petrology*, v. 29, p. 625-679.

McNeill, A. W., and Danyushevsky, L.V., 1996, Composition and crystallization temperatures of primary melts from Hole 896A basalts: evidence from melt inclusion studies. In: Alt, J.C., Kinoshita, H., Stoking, L.B., and Michael, P.J. (eds) *Proceedings of the Ocean Drilling Program, Scientific Results*, v. 148, p. 21-35.

Moore, J.G., 1965, Petrology of deep sea basalt near Hawaii: *American Journal of Science*, v. 263, p. 40-52.

Moore, J.G., and Evans, B.W., 1967, The role of olivine in the crystallization of the prehistoric Makaopuhi tholeiitic lava lake, Hawaii: *Contributions to Mineralogy and Petrology*, v. 15, p. 202-223.

Moore, J.G., and Koyanagi, R.Y., 1969, The October 1963 eruption of Kilauea Volcano, Hawaii: *United States Geological Survey Professional Paper*, 614-C, p. 1-13.

Muir, I.D., and Tilley, C.E., 1963, Contributions to the petrology of Hawaiian basalts, Part 2. The tholeiitic basalts of Mauna Loa and Kilauea, with chemical analyses by J.H. Scoon: *American Journal of Science*, v. 261, p. 111-128.

Murata, K. J., and Richter, D. H., 1966, Chemistry of the Lavas of the 1959-60 Eruption of Kilauea Volcano, Hawaii: United States Geological Survey Professional Paper 537-A.

Nichols, A.R.L., Carroll, M.R., and Höskuldsson, Á, 2002, Is Iceland hot spot also wet? Evidence from the water contents of undegassed submarine and subglacial pillow basalts: Earth and Planetary Science Letters, v. 202, p. 77-87.

Norman, M.D., and Garcia, M.O., 1999, Primitive magmas and source characteristics of the Hawaiian plume: petrology and geochemistry of shield picrites: Earth and Planetary Science Letters, v. 168, p. 27-44.

Norman, M.D., Garcia, M., Kamenetsky, V.S., and Nielson, R.L., 2002, Olivine-hosted olivine melt inclusions in Hawaiian picrites: Equilibration, melting and plume source characteristics: Chemical Geology, v.183, p.143-168, doi:10.1016/S0009-2541(01)00376-X.

Langmuir, C.H., Klein, E.M., and Plank, T., 1992, Petrological systematics of mid-ocean ridge basalts: constraints on melt generation beneath ocean ridges, in Mantle Flow and Melt generation at Mid-Ocean ridges, Geophysical Monogram Series, 71, edited by Morgan, J.P., Blackman, D.K., Sinton, J.M. AGU, Washington, D.C., p. 183-280.

Presnall, D.C., Gudfinnsson, G.H., and Walter, M.J., 2002, Generation of mid ocean ridge basalts at pressures from 1 to 7 GPa: Geochimica et Cosmochimica Acta, v. 66, p. 2073-2090.

Putirka, K.D., 2005, Mantle potential temperatures at Hawaii, Iceland, and the mid-ocean ridge system, as inferred from olivine phenocrysts: evidence for thermally driven mantle plumes: *Geochemistry Geophysics Geosystems*, 6, Q05L08, doi:10.1029/2005GC000915.

Quane, S.L., Garcia, M.O., Guillou, H., and Hulsebosch, T.P., 2000, Magmatic history of the East Rift Zone of Kilauea Volcano, Hawaii based on drill core SOH1: *Journal of Volcanology and Geothermal Research*, v. 102, p. 319-338.

Roeder, P.L., and Emslie, R.F., 1970, Olivine-liquid equilibrium: *Contributions to Mineralogy and Petrology*, 19, 275-89.

Richter, D.H., and Moore, J.G., 1966, Petrology of the Kilauea Iki Lava lake, Hawaii. United States Geological Survey Professional Paper, v. 537-B, p. 1-26.

Sigurdsson, I.A., Steinthorsson, S., and Grönvold, K., 2000, Calcium-rich melt inclusions in Cr-spinels from Borgarhraun, northern Iceland: *Earth and Planetary Science Letters*, v. 183, p. 15-26.

Sobolev, A.V., and Danyushevsky, L.V., 1994, Petrology and geochemistry of boninites from the north termination of the Tonga Trench: constraints on the generation conditions of primary high-Ca boninite magmas: *Journal of Petrology*, v. 35, p. 1183-1211.

Sobolev, A. V., and Nikogosian, I. K., 1994, Petrology of Long-Lived Mantle Plume Magmatism: Hawaii, Pacific, and Reunion Island, Indian Ocean: *Petrologiya*, v. 2, p. 131-168.

Sobolev, A.V., Danyushevsky, L.V., Dmitriev, L.V., Sushchevskaya, N.M., 1989, High-alumina magnesian tholeiite as the primary basalt magma at midocean ridge: *Geochemistry International*, v. 26, p. 128-133.

Sobolev, A.V., Hofmann, A.W., Sobolev, S.V., and Nikogosian, I.K., 2005, An olivine-free mantle source of Hawaiian shield basalts: *Nature*, v. 434, p. 590-597.

Takahashi, E., and Nakajima, K., 2002, Melting process in the Hawaiian plume: an experimental study: in Takahashi, E., Lipman, P.W., Garcia, M.O., Naka, J., and Aramaki, S., eds., *Hawaiian Volcanoes: Deep Underwater Perspectives*, Geophysical Monograph 128, 403-417.

Tilley, C.E., 1960, Kilauea magma: *Geological Magazine*, v. 97, p. 494-497.

Tilley, C.E., Thompson, R.N., Wadsworth, W.J., and Upton, B.G.J., 1971, Melting relations of some lavas of Réunion Island Indian Ocean: *Mineralogical Magazine*, v. 38, p. 344-352.

Toplis, M. J., 2005, The thermodynamics of iron and magnesian partitioning between olivine and liquid: criteria for assessing and predicting equilibrium in natural and experimental systems: *Contributions to Mineralogy and Petrology*, v. 149, p. 22-39.

Ulmer, P., 1989, The dependence of the Fe<sup>2+</sup> - Mg cation partitioning between olivine and basaltic liquid on pressure, temperature and composition: *Contributions to Mineralogy and Petrology*, v. 101, p. 261-273.

Wallace P. J., and Anderson, A.T., 1998, Effects of eruption and lava drainback on the H<sub>2</sub>O contents of basaltic magmas at Kilauea Volcano: *Bulletin of Volcanology*, v. 59, p. 327-344.

Wilkinson, J.F.G., and Hensel, H.D., 1988, The petrology of some picrites from Mauna Loa and Kilauea Volcanoes, Hawaii: *Contributions to Mineralogy and Petrology*, v. 98, p. 326-345.

Wright, T.L., 1971, Chemistry of Kilauea and Mauna Loa lava in space and time: *United States Geological Survey Professional Paper*, v. 735, p. 1-40.

Wright, T.L., and Fiske, R.S., 1971, Origin of the differentiated and hybrid lavas of Kilauea Volcano, Hawaii: *Journal of Petrology*, v. 12, p. 1-65.

Yaxley, G.M., and Green, D.H., 1998, Reactions between eclogite and peridotite: Mantle refertilization by subduction of oceanic crust: *Schweizerische Mineralogische und Petrographische Mitteilungen*, v. 78, p. 243-255.

## Figure Captions

### Figure 1

H<sub>2</sub>O versus K<sub>2</sub>O contents of glasses and melt inclusions from OIB 'hotspot' tholeiite series magmas. The H<sub>2</sub>O contents of the 1959 glasses are calculated using the observed eruption temperatures as a constraint (see text for discussion). The line "av. undegassed" is from the study of Wallace and Anderson (1998).

### Figure 2

FeO<sup>T</sup> versus MgO contents of whole rocks and glasses >8.5 wt% MgO from Kilauea Volcano, Hawaii. Symbols and lines as follows: small yellow circles, whole rock compositions from the 1959 Kilauea summit eruption; small open yellow circles, glass compositions from the 1959 Kilauea summit eruption; large open yellow circle, glass S-5g; large yellow circle, whole rock composition S-5; blue line, is an olivine control line representing olivine accumulation of ~Mg# 87; small black circles, other Kilauean whole rock compositions; open black circles, other Kilauean glass compositions; red diamonds, are the calculated 0.2 GPa parental liquid compositions (see Table 2); red lines, delineates the olivine addition paths (reverse of fractional crystallization); solid black line, is the locus of solidus melts for Hawaiian pyrolite composition (Green and Falloon, 1998) and the dash-dot black line is the locus of solidus melts for MORB pyrolite composition (Green and Falloon, 1998). Both lines are calculated using the equations of Herzberg and O'Hara (2002).

Data sources as follows: 1959 glasses, Helz (1987), Murata and Richter (1966); 1959 whole rocks, Murata and Richter (1966), Basaltic Volcanism Study Project (1981); Other

Kilauea glasses, Moore (1965), Clague et al. (1991), Clague et al. (1995), Garcia et al. (1996), Garcia et al. (2003); Other Kilauea whole rocks, Murata and Richter (1966), Moore (1965), Garcia et al. (2003); Clague et al. (1995), Basaltic Volcanism Study Project (1981), Garcia et al. (2000), Garcia et al. (1992), Richter and Moore (1966), Quane et al. (2000), Helz (1980), Mangan et al. (1995), Garcia et al. (1998), Moore and Koyanagi (1969), Wright (1971), Norman and Garcia (1999), Chen et al. (1996), Wilkinson and Hensel (1988), MacDonald and Eaton (1955), Muir and Tilley (1963), Aramaki and Moore (1969), Tilley (1960), Moore and Evans (1967), Wright and Fiske (1971), Gunn (1971).

### Figure 3

FeO<sup>T</sup> versus MgO wt% of MORB glass compositions. Symbols, lines and fields as follows: Blue square, parental liquid to MORB glass ODP896A (Table 2, no.8); green square, parental liquid to MORB glass D20-3 (Table 2, no.9); cyan square, parental liquid to MORB glass Vema, Mid-Atlantic Ridge (Table 2, no.10); blue circles, glass compositions from hole ODP896A, Cocos-Nazca (Danyushevsky, 2001); green circles, glass compositions from Siqueiros Fracture Zone, East Pacific Rise (Danyushevsky et al., 2003); magenta circles, glass compositions from the Australian Antarctic Discordance (AAD) (Danyushevsky, 2001); small black circles, MORB glasses from the study of Danyushevsky (2001); small open black circles, glasses from the Petdb data base with >9.5 wt% MgO as determined by electron microprobe analysis (petdb.ldeo.columbia.edu); solid blue, green and cyan lines are calculated liquid lines of descent for each respective parental liquid compositions undergoing crystal fractionation of olivine, clinopyroxene and plagioclase at 0.2 GPa. Calculations were performed using the software PETROLOG and the methods of Danyushevsky (2001). MORB glass field delineated by solid black line encompasses the range of FeO<sup>T</sup> and MgO

contents for 682 glasses from Danyushevsky (2001). MORB glass field delineated by dashed black line encompasses the range of  $\text{FeO}^{\text{T}}$  and MgO contents of 189 glasses with  $>9.5$  wt% MgO as determined by electron microprobe analysis from the Petdb database ([petdb.ldeo.columbia.edu](http://petdb.ldeo.columbia.edu)). Temperatures of MORB parental liquid compositions are calculated using the olivine geothermometer of Ford et al. (1983) at 0.2 GPa (see text and Table 2 for details). Dashed line at 8 wt% MgO is the MORB reference MgO content after Klein and Langmuir (1987).

#### Figure 4

Projection of partial melting trends for Hawaiian pyrolite composition (dashed curves, 0.5 – 3.0 GPa) i.e. liquid compositions lying on lherzolite (ol + opx + cpx + spinel) and harzburgite (ol + opx + Cr-spinel) within the normative "basalt tetrahedron" (Falloon and Green, 1998; Falloon et al., 1998, Falloon unpubl data). Projections are from olivine (a) and diopside (b). Glasses and calculated parental liquid compositions (P) are from Tables 2 and 3. Kilauea picrite whole rock (K. picrite wr) and melt inclusions (K. picrite ml) are from Norman and Garcia (1999) and Norman et al. (2002).

#### Figure 5

Projection of partial melting trends for MORB pyrolite (thick solid lines, 0.8 – 2.5 GPa) and MM-3 lherzolite composition (thin dashed lines, 1.0-2.0 GPa) within the normative "basalt tetrahedron" (Falloon and Green, 1998; Falloon et al., 1999; Falloon et al., 2001; appendix 1; Falloon unpubl data). Solid line with arrow is the locus of liquids in equilibrium with

plagioclase lherzolite (ol + opx + cpx + plag  $\pm$  Cr-spinel) at 1 GPa – such liquids are low in normative diopside and olivine.

Projections are from olivine (a) and diopside (b). Glasses and calculated parental liquid compositions (P) are from Tables 2 and 3. Data for ODP896A, Siqueiros and Vema glasses (Danyushevsky unpubl data). Coloured arrows represent olivine control lines from the respective parental liquid compositions.

**TABLE 1. GLASS COMPOSITIONS CHOSEN FOR STUDY**

No. Sample name	1 F-3g	2 S-5g	3 57-11c	4 57-13g	5 57-15D	6 57-9F	7 182-7	8 REg	9 ODP896A	10 D20-3	11 Vema	12 NO42
SiO <sub>2</sub>	50.12	48.69	48.83	48.7	49.59	51.65	51.24	47.96	49.07	49.15	49.66	48.32
TiO <sub>2</sub>	3.52	2.47	1.92	1.9	2.09	2.27	2.17	2.98	0.64	0.96	0.86	0.78
Al <sub>2</sub> O <sub>3</sub>	13.36	12.39	11.38	10.99	12.03	13.43	13.4	14.2	16.08	16.99	17.77	15.81
Fe <sub>2</sub> O <sub>3</sub>	2.49	1.52	1.6	1.52	1.38	1.04	1.36	1.78	0.67	0.60	0.49	1.06
FeO	10.0	10.02	11.25	10.53	9.98	7.93	9.30	9.3	8.53	7.61	6.61	8.41
MnO	0.18	0.18	N.D.	N.D	N.D	N.D	0.16	0.2	0.12	0.13	0.13	0.18
MgO	5.68	10.12	13.29	14.92	12.53	9.73	8.42	7.09	9.44	9.88	9.51	9.80
CaO	9.61	10.95	9.01	8.67	9.46	10.63	10.7	11.3	13.67	12.13	12.45	13.79
Na <sub>2</sub> O	2.57	2.03	1.65	1.63	1.77	2.03	2.16	2.62	1.62	2.41	2.32	1.63
K <sub>2</sub> O	0.71	0.48	0.3	0.32	0.33	0.36	0.31	0.76	0.02	0.02	0.06	0.04
P <sub>2</sub> O <sub>5</sub>	0.39	0.24	0.20	0.19	0.21	0.23	0.19	0.29	0.03	0.05	0.05	0.09
Cr <sub>2</sub> O <sub>3</sub>	N.D	N.D	N.D	N.D	N.D	N.D	N.D	N.D	0.07	N.D	N.D	N.D
H <sub>2</sub> O	1.38	0.93	0.58	0.63	0.64	0.7	0.6	1.52	0.05	0.07	0.10	0.10
Mg#	50.3	64.3	67.8	71.6	69.1	68.6	61.7	57.6	66.4	69.8	71.9	67.5
Temp	1064	1190	1269	1301	1253	1189	1157	1100	1200	1223	1207	1202
Oliv Eq	74.8	85.0	86.6	88.7	87.4	87.1	82.9	81.1	86.2	88.3	89.3	86.9

*Notes:* Data sources: glasses 1 and 2, Murata and Richter (1966); glasses 3-6, Clague et al. (1995); glass 7, Garcia et al. (1985); glass 8, Tilley et al. (1971); glass 9, glass ODP Leg 896A-27R-1, 124-130, pc.15 (McNeill and Danyushevsky, 1996); glass 10, Danyushevsky et al. (2003); glass 11, Sobolev et al. (1989); glass 12, Sigurdsson et al. (2000). Fe<sub>2</sub>O<sub>3</sub> and FeO contents of all glasses have been calculated at QFM+0.5 log units (glasses 1-8, 12) or QFM-0.5 log units (glasses 9-11) at 0.2 GPa using the model of Borisov and Shapkin (1990). H<sub>2</sub>O contents are either analysed in the glass (no.9-11) or calculated from K<sub>2</sub>O contents (no.1-8, 12, see text for discussion). Temp, refers to the calculated olivine liquidus temperature at 0.2 GPa using the models of Ford et al. (1983) and Falloon and Danyushevsky (2000). Oliv Eq, refers to the calculated equilibrium olivine composition at the 0.2 GPa liquidus temperature. "N.D." refers to no data. All calculations performed with software PETROLOG (Danyushevsky, 2001).

**TABLE 2. CALCULATED MODEL PARENTAL LIQUIDS AT 0.2 GPA**

No. Sample Name	Kilauea					Mauna Loa	Reunion	MORB			Iceland
	1	2	3	4	5	6	7	8	9	10	11
	S-5g	57-11c	57-13g	57-15D	57-9F	182-7	REg	ODP896A	D20-3	Vema	NO42
SiO <sub>2</sub>	47.24	47.53	48.01	48.48	50.44	48.74	46.23	47.70	48.29	49.36	47.00
TiO <sub>2</sub>	2.03	1.62	1.73	1.83	2.02	1.67	2.31	0.54	0.86	0.83	0.64
Al <sub>2</sub> O <sub>3</sub>	10.21	9.59	10.04	10.54	11.95	10.30	10.98	13.46	15.25	17.17	13.03
Fe <sub>2</sub> O <sub>3</sub>	1.58	1.80	1.64	1.51	1.12	1.54	1.51	0.85	0.69	0.51	1.40
FeO	9.96	10.77	10.26	9.78	8.05	9.38	9.91	8.56	7.69	6.68	8.15
MnO	0.15	N.D	N.D	N.D	N.D	0.12	0.15	0.10	0.12	0.12	0.15
MgO	16.79	18.80	17.86	17.00	14.00	17.53	16.17	15.86	13.93	10.86	16.75
CaO	9.03	7.59	7.92	8.28	9.46	8.22	8.73	11.44	10.88	12.03	11.37
Na <sub>2</sub> O	1.67	1.39	1.49	1.55	1.81	1.66	2.02	1.36	2.16	2.24	1.34
K <sub>2</sub> O	0.39	0.25	0.29	0.29	0.32	0.24	0.59	0.02	0.02	0.06	0.03
P <sub>2</sub> O <sub>5</sub>	0.20	0.17	0.18	0.18	0.20	0.15	0.22	0.03	0.04	0.05	0.07
Cr <sub>2</sub> O <sub>3</sub>	N.D	N.D	N.D	N.D	N.D	N.D	N.D	0.06	N.D	N.D	N.D
H <sub>2</sub> O	0.76	0.49	0.57	0.56	0.62	0.46	1.18	0.04	0.06	0.10	0.08
Mg#	75.0	75.7	75.6	75.6	75.6	76.9	74.4	76.8	76.3	74.3	78.6
Temp	1335	1372	1355	1341	1286	1354	1323	1351	1320	1243	1361
Oliv Eq	90.70	90.70	90.70	90.70	90.70	91.30	90.65	91.60	91.50	90.50	92.40
% Oliv	17.6	15.7	8.6	12.4	11.0	23.1	22.7	16.3	10.3	3.4	17.5

Notes: Data sources, Temp and Oliv Eq as for Table 1. %Oliv, refers to the amount of olivine added in incremental steps to obtain equilibrium with the target olivine compositions (see text for discussion). "N.D." refers to no data. All calculations performed with software PETROLOG (Danyushevsky, 2001) at conditions and parameters as listed in the notes to Table 1.

**TABLE 3. COMPARISON OF MODEL  
KILAUEA PARENTAL LIQUIDS WITH  
EXPERIMENTAL MELT COMPOSITIONS  
FROM HW-40 AT 2 GPA UNDER  
ANHYDROUS CONDITIONS**

	T-2018	57-15D	57-13g	T-650
SiO <sub>2</sub>	48.15	48.48	48.01	50.19
TiO <sub>2</sub>	2.35	1.83	1.73	1.74
Al <sub>2</sub> O <sub>3</sub>	10.76	10.54	10.04	8.61
Fe <sub>2</sub> O <sub>3</sub>	N.A.	1.51	1.64	N.A.
FeO	10.16	9.78	10.26	9.34
MgO	16.27	17.00	17.86	19.96
CaO	9.38	8.28	7.92	7.40
Na <sub>2</sub> O	1.87	1.55	1.49	1.40
K <sub>2</sub> O	0.39	0.29	0.29	0.32
P <sub>2</sub> O <sub>5</sub>	N.D.	0.18	0.18	N.D.
H <sub>2</sub> O	N.D.	0.56	0.57	N.D.
Temp	1500	1506	1523	1550
Mg#	74.1	75.6	75.6	79.2

*Notes:* Data sources: experimental glasses T-2018 and T-650 (Falloon et al., 1988). Temp, refers to the anhydrous olivine liquidus temperatures calculated at 2 GPa using the model of Ford et al. (1983) and assuming all Fe as Fe<sup>2+</sup>. "N.D." refers to no data and "N.A." refers to not applicable.

**TABLE 4. COMPARISON OF MODEL  
ODP896A PARENTAL LIQUID WITH  
EXPERIMENTAL MELTS FROM MM-3  
AND MPY-87 AT 2 GPa UNDER  
ANHYDROUS CONDITIONS**

	T-4107	ODP896A	T-4190
SiO <sub>2</sub>	47.75	47.7	48.30
TiO <sub>2</sub>	0.61	0.54	0.74
Al <sub>2</sub> O <sub>3</sub>	13.96	13.46	13.40
Fe <sub>2</sub> O <sub>3</sub>	N.A.	0.85	N.A.
FeO	8.49	8.56	8.01
MnO	N.D.	0.10	0.15
MgO	15.37	15.86	15.95
CaO	11.83	11.44	11.48
Na <sub>2</sub> O	1.40	1.36	1.57
K <sub>2</sub> O	N.A.	0.02	N.A.
P <sub>2</sub> O <sub>5</sub>	N.A.	0.03	N.A.
Cr <sub>2</sub> O <sub>3</sub>	0.34	0.06	0.36
H <sub>2</sub> O	N.D.	0.04	N.D.
Temp	1460	1474	1475
Mg#	76.3	76.8	78.0

*Notes:* Data sources: experimental glasses T-4107 and T-4190 (see appendix Table A3). Temp, refers to the anhydrous olivine liquidus temperatures calculated at 2 GPa using the model of Ford et al. (1983) and assuming all Fe as Fe<sup>2+</sup>. "N.D." refers to no data and "N.A." refers to not applicable.

**TABLE 5. PETROGENETIC SUMMARY AND MODEL CALCULATIONS OF MANTLE POTENTIAL TEMPERATURES**

Parent	T (0.2 GPa)	T (final)	ΔT (adiabat)	P (final)*	P (final)†	MgO wt%	H <sub>2</sub> O wt%	Oliv Mg# (0.2 GPa)	Oliv Mg# (final)	Mantle Residue	F%	T <sub>p</sub>
<b>MORB</b>												
ODP896A	1351	1441	36	2.00	2.01	15.86	0.04	91.6	90.5	Sp LHz	0.20	1488
Siqueiros	1320	1400	32	1.80	1.65	13.93	0.06	91.5	90.4	Sp LHz	0.13	1425
Vema	1243	1286	16	1.10	1.16	10.86	0.10	90.5	89.8	Sp LHz	0.13	1318
<b>Iceland</b>												
NO42	1361	1468	41	2.40	2.34	16.75	0.08	92.4	91.3	Hz	0.17	1501
<b>Hawaii</b>												
<b>Kilauea</b>												
S-5g	1335	1436	41	2.20	2.27	16.79	0.76	90.7	89.4	Hz	0.33 <i>0.12</i>	1524 <i>1454</i>
57-13g	1355	1451	39	2.10	2.16	17.86	0.57	90.7	89.5	Hz	0.40 <i>0.14</i>	1563 <i>1477</i>
57-15D	1341	1422	33	1.80	1.93	17.00	0.56	90.7	89.7	Hz	0.38 <i>0.14</i>	1531 <i>1451</i>
57-11c	1372	1488	47	2.50	2.44	18.8	0.49	90.7	89.3	Hz	0.44 <i>0.16</i>	1610 <i>1516</i>
57-9F	1286	1326	16	1.00	1.23	14.00	0.62	90.7	90.1	Hz	0.34 <i>0.12</i>	1429 <i>1356</i>
<b>Mauna Loa</b>												
182-7	1354	1445	37	2.00	1.92	17.53	0.46	91.3	90.3	Hz	0.42 <i>0.15</i>	1565 <i>1475</i>
<b>Reunion</b>												
REg	1323	1440	48	2.50	2.52	16.17	1.18	90.65	89.1	Hz	0.26 <i>0.09</i>	1502 <i>1445</i>
<p><i>Notes:</i> Abbreviations as follows: T (0.2 GPa) refers to the calculated olivine crystallization temperature of the parental liquids at 0.2 GPa (see Table 2); T (final) refers to the calculated olivine crystallization at the pressure of mantle equilibration [see column P (final)*]; ΔT (adiabat), refers to the difference between the temperature of the parental liquid if it rises to the surface along a liquid adiabat and the olivine crystallization temperature at 0.2 GPa, i.e., it is a measure of possible superheat of the magma; P (final)*, refers to the pressure of mantle equilibration estimated from the position of the parental liquid compositions within the normative tetrahedron (see text for discussion); P (final)†, refers to the pressure of mantle equilibration estimated by the empirical calibration of Alabarede (1992). MgO wt%, refers to the MgO wt% of the calculated parental liquids (Table 2); H<sub>2</sub>O wt%, refers to the H<sub>2</sub>O wt% of the calculated parental liquids (Table 2); Oliv Mg# (0.2 GPa), refers to the calculated equilibrium liquidus olivine at 0.2 GPa (Table 2); Oliv Mg# (final), refers to the calculated equilibrium liquidus olivine at the pressure of mantle equilibration [column P (final)*]; Mantle Residue, refers to the residue mineralogy at the pressure and temperature of mantle equilibration, Sp LHz = spinel lherzolite, Hz = harzburgite ± Cr-spinel; F%, refers to the degree of partial melting estimated for the parental compositions (see text for discussion). Values in italics for F% and for T<sub>p</sub> refer to calculations based on a refractory Hawaiian Pyrolite composition (harzburgite + 10% picrite); T<sub>p</sub> is the calculated mantle potential temperature derived from <math>[T_{\text{final}} + \Delta T_{\text{fusion}} - \Delta T_{\text{solid adiabat}}]</math> where <math>\Delta T_{\text{fusion}}</math> is the latent heat of melting based on the model source and derived F%, and <math>dT_{\text{solid adiabat}}</math> is the adiabatic cooling from P<sub>final</sub> to surface along the olivine adiabat.</p>												

**TABLE A1. STARTING COMPOSITIONS USED**

Composition	SiO <sub>2</sub>	TiO <sub>2</sub>	Al <sub>2</sub> O <sub>3</sub>	FeO	MnO	MgO	CaO	Na <sub>2</sub> O	Cr <sub>2</sub> O <sub>3</sub>
MM-3	45.50	0.11	3.98	7.18	0.13	38.30	3.57	0.31	0.68
ODP896A	47.90	0.57	13.87	9.29	0.10	15.15	11.60	1.40	0.07
ARP74	50.82	0.83	15.20	8.12	N.A.	10.25	12.21	2.09	N.A.

Notes: "N.A." refers to not applicable.

**TABLE A2. EXPERIMENTAL RUN DATA ON PERIDOTITE REACTION EXPERIMENTS**

No.	Run No.	Run Temp (°C)	Time (hrs, mins)	wt% basalt	ML/ML <sub>f</sub>	Basalt composition	Phase assemblage
<b>1.8 GPa</b>							
1	T-4154	1425	24	0.26	0.68	ODP896A	Ol+Opx+Cpx+L
2	T-4153	1450	24	0.31	0.61	ODP896A	Ol+Opx+L
<b>2.0 GPa</b>							
3	T-4107	1450	24	0.44	0.81	ODP896A	Ol+Opx+Cpx+L
4	T-4190	1450	24	0.37	0.68	ARP74	Ol+Opx+L
5	T-4191	1475	24	0.30	0.56	ARP74	Ol+Opx+L

*Notes:* Run Temp (°C) refers to the recorded temperature of the experiment; wt% basalt refers to the wt. fraction of basalt composition added as a layer in the peridotite reaction experiments; ML/ML<sub>f</sub> refers to the wt fraction ratio between the initial amount of added basalt component to the final amount of melt component in the experiment obtained by mass balance (Table A3), values less than 1 indicate that the peridotite component has melted and contributed to the melt phase during reaction. Thus the final equilibrium assemblage is the result of a melting and reaction process not a crystallization and reaction process (values >1). Phase assemblage abbreviations are as follows: Ol, olivine; Opx, orthopyroxene; Cpx, clinopyroxene.

**TABLE A3. COMPOSITIONS OF EXPERIMENTAL RUN PRODUCTS**

Run no.	Phase	MB BC	MB MM-3	Type	SiO <sub>2</sub>	TiO <sub>2</sub>	Al <sub>2</sub> O <sub>3</sub>	Cr <sub>2</sub> O <sub>3</sub>	FeO	MnO	MgO	CaO	Na <sub>2</sub> O
<b>1.8 GPa</b>													
T-4154	Olivine	0.424(4)	0.55(1)	N.A.	40.81	N.D.	N.D.	N.D.	8.52	0.21	50.11	0.34	N.D.
	Orthopyroxene	0.17(1)	0.22(3)	N.A.	54.51	0.07	4.86	1.25	5.07	0.1	31.29	2.76	0.09
	Clinopyroxene	0.02(1)	0.06(3)	N.A.	52.37	0.09	5.66	1.47	4.55	0.06	23.37	12.08	0.35
	Glass	0.38(1)	0.17(2)	N.A.	48.09	0.65	14.16	0.38	8.12	0.12	14.8	12.09	1.49
	Residual	<b>0.0217</b>	<b>0.1699</b>										
T-4153	Olivine	0.395(6)	0.56(1)	N.A.	41.43	N.D.	N.D.	N.D.	7.94	0.12	50.16	0.33	N.D.
	Orthopyroxene	0.09(1)	0.18(2)	N.A.	54.51	0.07	4.86	1.25	5.07	0.1	31.29	2.76	0.09
	Glass	0.51(1)	0.25(1)	N.A.	48.6	0.56	12.83	0.54	8.21	0.11	16.31	11.51	1.23
	Residual	<b>0.0552</b>	<b>0.1662</b>										
<b>2.0 GPa</b>													
T-4107	Olivine	0.306(5)	0.56(2)	N.A.	40.9	N.D.	N.D.	N.D.	9.27	N.D.	49.68	0.15	N.D.
	Orthopyroxene	0.11(2)	0.20(5)	N.A.	54.93	N.D.	4.63	0.69	5.51	N.D.	31.78	2.45	N.D.
	Clinopyroxene	0.04(2)	0.05(5)	N.A.	51.92	N.D.	5.47	1.04	4.97	N.D.	24.88	10.02	0.17
	Glass	0.54(1)	0.20(3)	N.A.	47.75	0.61	13.96	0.34	8.49	N.D.	15.37	11.83	1.4
	Residual	<b>0.0341</b>	<b>0.3622</b>										
T-4190	Olivine	0.263(4)	0.55(1)	A(3)	41.3(3)	N.D.	N.D.	0.25(2)	8.4(1)	0.10(4)	50.2(3)	0.31(0)	N.D.
	Orthopyroxene	0.185(7)	0.21(2)	A(3)	54.87(9)	0.09(2)	4.3(1)	1.1(1)	4.8(1)	0.13(4)	32.0(1)	2.5(1)	0.12(1)
	Glass	0.548(5)	0.23(2)	A(5)	48.3(1)	0.74(4)	13.4(1)	0.36(2)	8.0(1)	0.15(4)	15.95(7)	11.48(9)	1.57(3)
	Residual	<b>0.0256</b>	<b>0.2603</b>										
T-4191	Olivine	0.324(6)	0.56(1)	A(3)	41.3(3)	N.D.	N.D.	0.36(2)	8.0(1)	0.10(2)	50.3(7)	0.5(3)	N.D.
	Orthopyroxene	0.14(10)	0.17(2)	A(3)	55.6(2)	0.07(4)	3.4(2)	0.88(7)	4.83(7)	0.09(4)	33.0(1)	2.02(2)	0.09(2)
	Glass	0.535(8)	0.26(1)	A(5)	48.8(2)	0.66(3)	12.66(7)	0.43(3)	7.8(2)	0.15(2)	17.20(5)	10.8(1)	1.37(2)
	Residual	<b>0.0636</b>	<b>0.1447</b>										

Notes: Mass balance in weight fraction was performed using least squares linear regression using the software PETMIX and "Residual" refers to the square of the sum of the residuals. "MB BC" refers to mass balance using the bulk composition of the experiment whereas "MB MM-3" refers to mass balance using the peridotite composition MM-3 only. Numbers in parentheses next to each analysis or mass balance are 1 $\sigma$  in terms of the last units cited; e.g., 0.540(9) refers to 0.540 $\pm$ 0.009 "A" indicates that the analysis is an average with the number of analyses used to calculate the average given in the parentheses. "N.D." refers to not determined and "N.A." refers to not applicable.

Figure 1

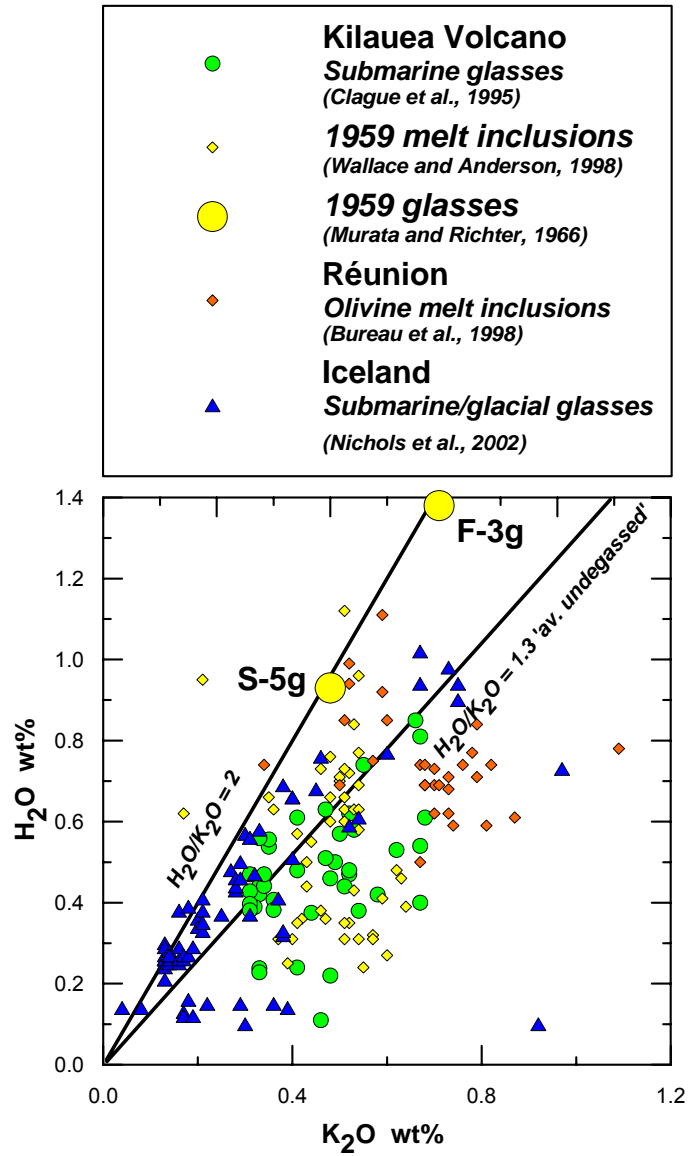


Figure 2

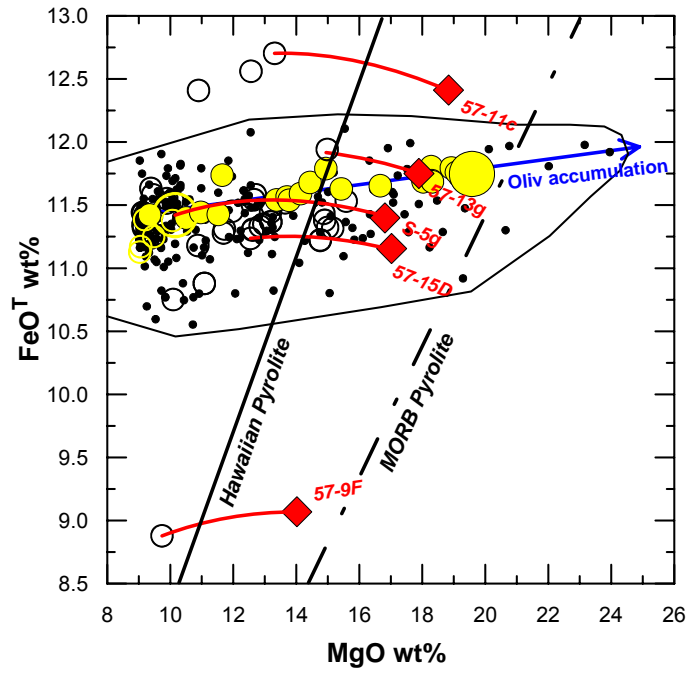


Figure 3

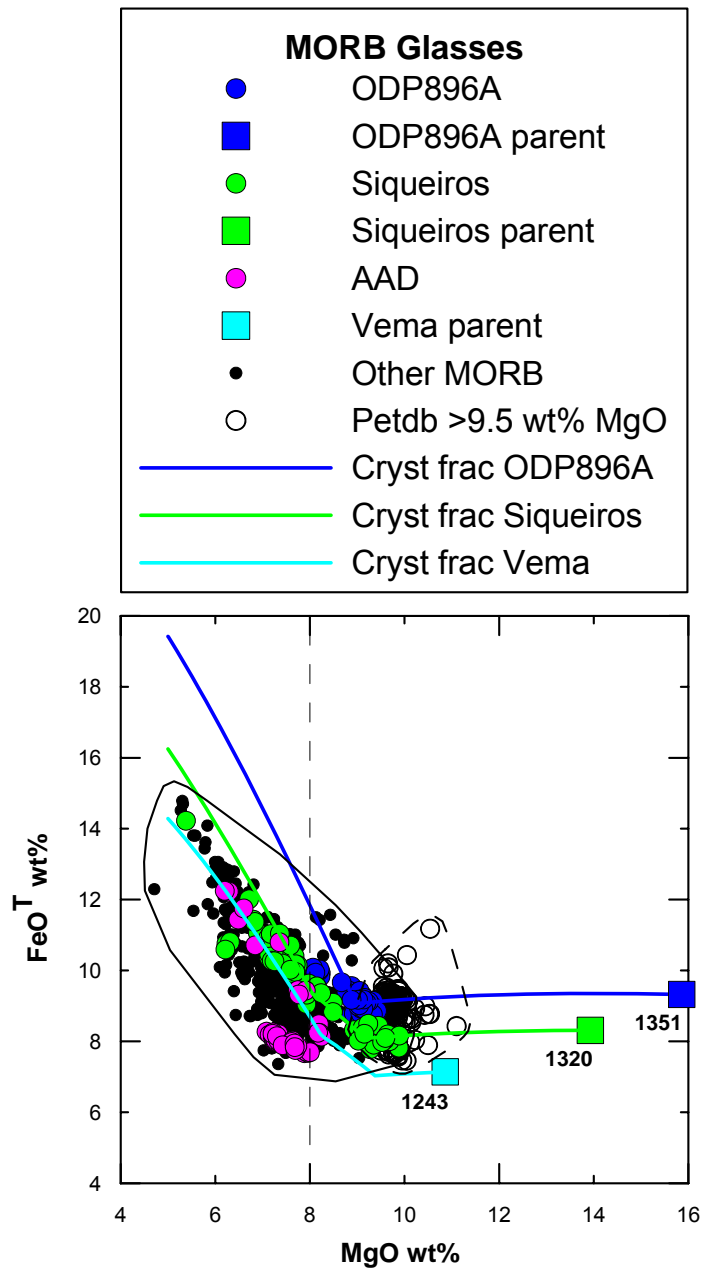


Figure 4

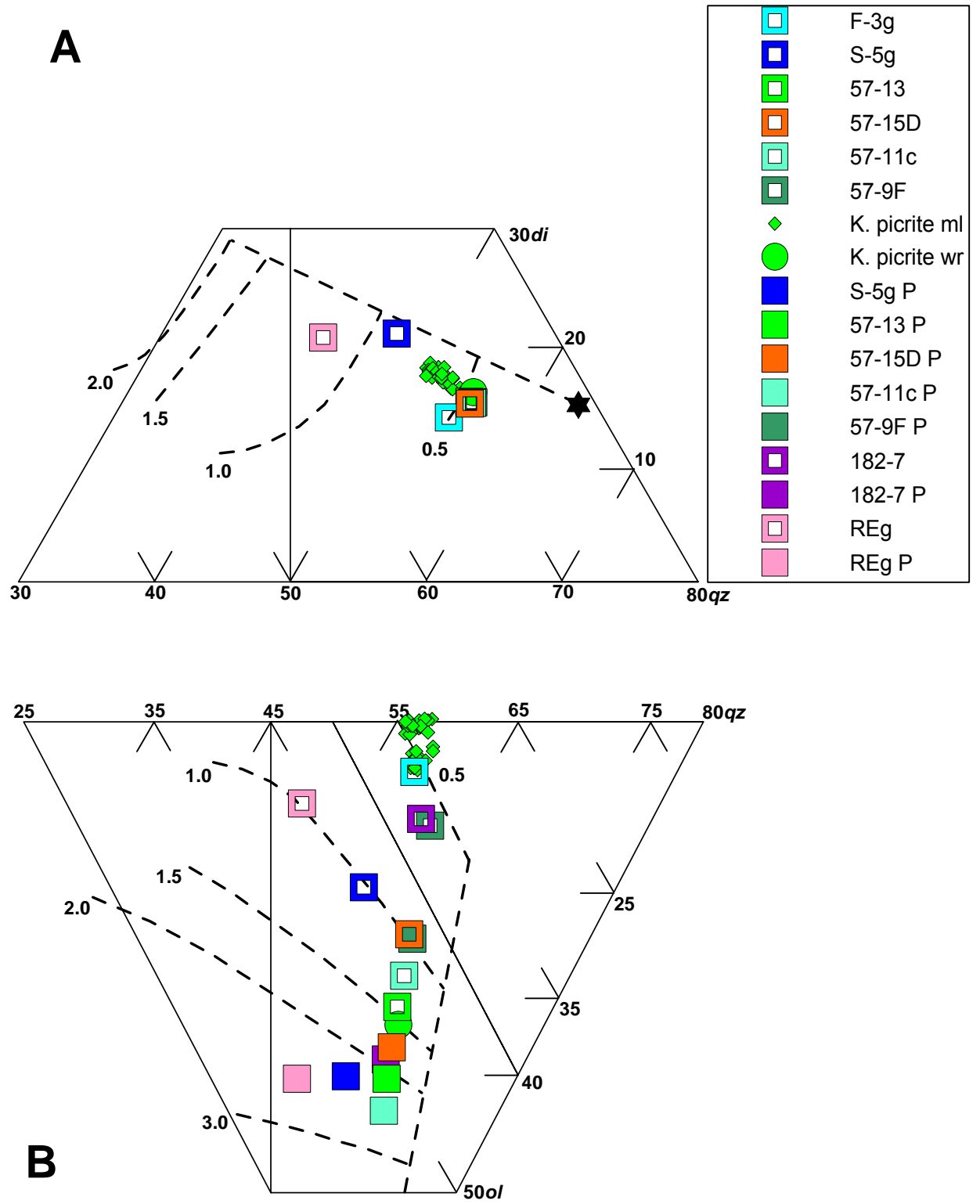


Figure 5

